Universidade de Aveiro Departamento de Engenharia Cerâmica e do Vidro
2011

Oleg Fedotov

Relevância da carga superficial na adsorção de proteínas em biomateriais

Relevance of surface charge on protein adsorption onto biomaterials

Universidade de Aveiro Departamento de Engenharia Cerâmica e do Vidro
2011

Oleg Fedotov

Relevância da carga superficial na adsorção de proteínas em biomateriais

Relevance of surface charge on protein adsorption onto biomaterials

Dissertação apresentada à Universidade de Aveiro para cumprimento dos requisitos necessários à obtenção do grau de Mestre em Materiais e Dispositivos Biomedicos, realizada sob a orientação científica da Doutora Maria Helena Figueira Vaz Fernandes e co-orientação científica da Doutora Paula Maria Lousada Silveirinha Vilarinho do Departamento de Engenharia Cerâmica e do Vidro da Universidade de Aveiro

o júri

presidente

Prof. Doutor Francisco Manuel Lemos Amado, Universidade de Aveiro
Professor Associado da Universidade de Aveiro

Profª. Doutora Maria Ascensão Ferreira da Silva Lopes, Universidade do Porto
Professora Auxiliar da Universidade de Porto (Arguente)

Profª. Maria Helena Figueira Vaz Fernandes, Universidade de Aveiro
Professora Associada da Universidade de Aveiro (Orientadora)

Profª. Doutora Paula Maria Lousada Silveirinha Vilarinho, Universidade de Aveiro
Professora Associada da Universidade de Aveiro (Co-orientadora)

agradecimentos

A execução deste trabalho foi conseguida graças ao contributo de diversas pessoas e entidades. Mesmo correndo o risco de não as referir a todas, gostava de manifestar os meus agradecimentos:

- À minha família, pelo apoio moral concedido durante a realização deste trabalho.
- Aos meus orientadores da Universidade de Aveiro, Doutora Maria Helena Figueira Vaz Fernandes e Doutora Paula Maria Lousada Silveirinha Vilarinho, pelo acompanhamento.
- Natália Braz Barroca pela ajuda em realização deste trabalho.
- Rui Miguel Pinheiro Vitorino do Departamento da Química da Universidade de Aveiro pelo acolhimento no laboratório para a realização das experiencias.

palavras-chave

carga superficial, hidrxiapatite, biovidro V-7, PLLA, zeta potencial, albumina, adsorção de albumina

resumo

O principal objectivo do presente trabalho consiste em estudar o comportamento de adsorção de uma proteína específica - Albumina de Soro Bovino (BSA) - sobre a superfície de três materiais (hidroxiapatita comercial, um biovidro V7 e ácido poli-L-láctico) que podem ser utilizados em aplicações biomédicas para fins de implantação.

O estudo comparativo foi baseado em medição do zeta potencial e na determinação da quantidade de proteína BSA adsorvida sobre a superfície dos biomateriais em estudo sob diferentes condições (pH, concentração de BSA e tempo de incubação).

keywords surface charge, hydrxyapatite, bioglass V-7, PLLA, zeta potential, albumin, albumin adsorption

abstract The main purpose of the present work is to study and compare the adsorption behaviour of a specific protein – Bovine Serum Albumin (BSA) - onto the surface of three materials (commercial hydroxyapatite, a bioglass V7 and poly-L-lactide acid) that can be used in biomedical applications for implant purposes. The comparative study was based on zeta potential measurements and on the determination of the amount of BSA protein adsorbed on the surface of the biosubstrates under different conditions of pH, BSA concentration and time of incubation.

Table of Contents

1. Introduction

The bone regeneration process, the interaction between implant and human plasma begins from the adsorption of proteins to the surface of the material.

The main objective of this work is to study the interaction of various surfaces of biomaterials with a protein (in this case albumin). To accomplish this study three materials were selected: hydroxyapatite (HA), a bioglass produced in our laboratory, designated by V7, and poly-L-lactide acid (PLLA). All these materials have a great biological interest: HA is a bone constituent, bioglass V7 is a glass that exhibited *in vitro* bioactivity in accellular immersion tests and PLLA is an implantable material extensively used in Medicine. The determination of surface charge by measuring the zeta potential under different conditions (pH, added protein concentration and time of immersion) and protein adsorption onto the surface of materials were essential points to assess during this work.

The surface charge of biomaterials plays a great role in the process of bone remodeling and regeneration, so understanding this phenomenon can help to create the adequate conditions for bone regeneration.

The environment of a healthy tissue has pH of 7.4 and inflammatory tissue has pH of 4.5. These were the two conditions studied for a better understanding of the significance of the interactions of the surface charge of the material and albumin.

Bovine serum albumin (BSA) was the chosen protein to conduct the experimental work that consists in the study of the protein adsorption on the surface of the material (HA, bioglassV7, and PLLA) due to its relatively low cost, availability, solubility in aqueous medium, homogeneity and to the fact of being the most abundant protein in the human plasma (concentration of 38-50 $g.L^{-1}$).

2. Theoretical background

In this section the structure and process of bone regeneration and the basic factors that influence the protein adsorption processes will be presented. Further the definition of the protein, its structure and functions will be described. Emphases will be given to the explanation of the basic concepts of zeta potential, contact angle and particle size.

2.1. Bone composition

Bone is defined as a metabolically active tissue that suffers a lot of chemical and physical processes [1].

Bone is made of two types of tissues: trabecular and cortical [2]. The trabecular bone consists of medulla and blood vessels. The medulla is the medium for cells and differentiated cells, while the blood vessels allow metabolic changes and traffic signals to keep good bone physiology.

The cortical bone is constituted by an inorganic phase (60-70% dry weight), an organic phase (~ 35%) and water (5-8%). The inorganic phase corresponds to nanocrystals of hydroxyapatite (HA), and the organic phase consists of nanofibers of collagen type I (90%), non-collagenous protein (10%) and the bone cells [3]. The extracellular matrix is formed by such bone cells as the osteoblasts, osteocytes and osteoclasts that are responsible for the formation, maintenance and resorption of the bone, respectively. HA crystals are included in the fibrils collagen (Figure 1.1).

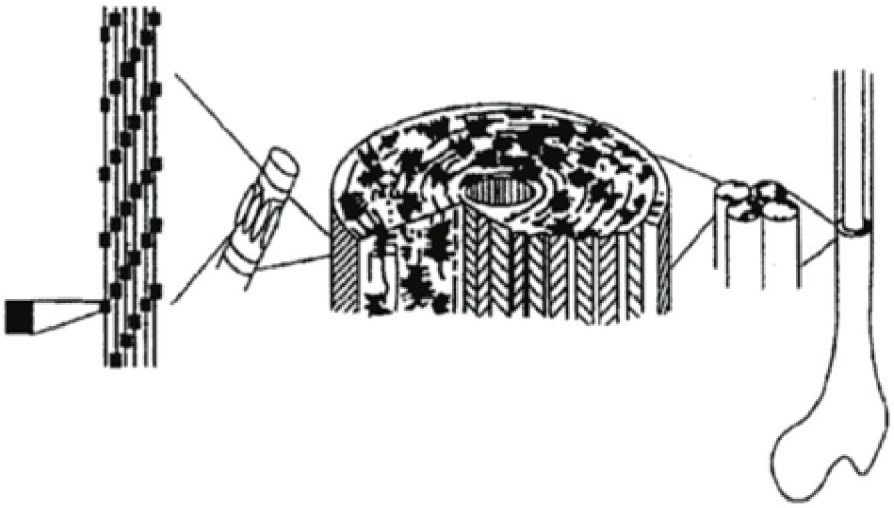

Figure 1.1: Organization of compact bone (adapted from [3]).

The bone tissue has several functions [3]:

- mechanical, as it serves as a support for muscles, ligaments and tendons and allows the movement of skeleton;
- protection of organs and tissues;
- hematopoietic as it assumes the formation of the blood;
- and metabolic function that provides a reservoir for mineral homeostasis of Ca and PO_4.

Bone is a regenerable tissue, so old cells can be replaced by new ones as schematically represented in Figure 1.2. This process is defined as bone remodeling cycle [4]. In the bone regeneration process local regions of the bone

are destroyed by osteoclasts as a result of fracture, microdamage or normal aging process and then rebuilt by osteoblasts [5].

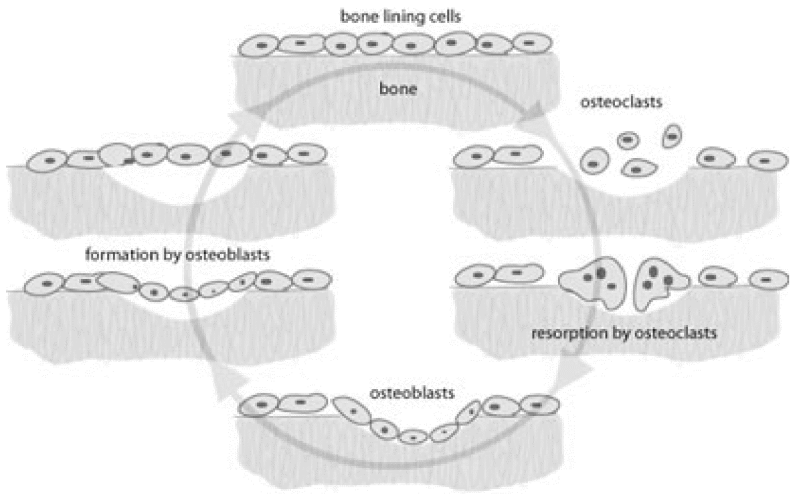

Figure 1.2: Bone remodeling cycle [6].

Every year, approximately one million people need bone grafts to repair bone defects that occur as a result of illness or accidents. The implantation has important socio-economic consequences like increase of life expectancy and quality.

Whenever possible autologous and homologous grafts are the preferred strategies in clinical implantation.

In the autologous grafts bone is taken from the patient that is at the same time the recipient [7]. It is considered the best treatment because the removed bone contains osteogenic cells and osteoinductor factors like growth factors. The main drawback of this strategy is related to the fact that the amount of bone that can be taken from donor side is limited [8].

In the homologous grafts the bone is taken from a donor that is not the recipient. This form of graft has the disadvantage of a high probability of immune reaction from the recipient side [9].

Metal and ceramic materials are the most used synthetic bone implants, instead of autologous and homologous grafts, some of them due to the biocompatibility, others due to the mechanical properties [10, 11].

2.2. The relevance of surface charge in the bone regeneration process

Wolff [12] has developed the hypothesis that the bone, as a dynamic body, is adaptative to mechanical environment. The "Wolff's Law" reflects the ability of the bone to adapt to mechanical stresses and in this way explains certain phenomena such as the decrease in bone density during a long mission of astronauts or the increase of sportsmen´s bone density in response to their training. The study made by Pontzer [13] also concluded that the bone adapts to compressive forces as Wolff law indicates.

Another factor that influences the bone regeneration process is the condition of the blood vessels due to the metabolic rate of regeneration cells [14].

Osteocytes and osteoblasts cells are responsible for bone's adaptability, but till now there is no answer with respect to the driving force of this behavior. One of the possible explanations for this phenomenon was found in 1960 and is based on the piezoelectric (use of local stresses) properties of collagen due to which osteocytes can detect areas of greater stress [12]. Also it was concluded that the characteristics of collagen fibrils are important in the identification of the area that requires the regeneration [15]. The basic concept of this theory explains that the use of local stresses along the fibers of collagen can provide increase of bone cells that regenerate bone tissue. [16].

Adhesion is one of the parameters that can influence the cell capacity to proliferate or differentiate the bone regeneration cells [17]. This process determines the failure or success of the implant in service. This knowledge was applied to produce ceramic implants with electrically charged surface to attract higher amounts of bone regeneration cells [18].

There is a great number of studies on the influence of the implant's surface electrical charge on the bone regeneration process. According to Lu *et al.* [19] the presence of negative charges on the surface of materials in *vitro* contributes to the formation of apatite layer, while in vivo, it increases the proliferation of osteoblasts and bone growth.

A study in *vivo* made by Brendel *et al.* [20] revealed the formation of bone bind after the insertion of the negatively charged polymeric implants to the rats.

Dekhtyar *et al.* [21] performed another study and verified the formation of bone around the electrically charged implants, while the implants without charge didn´t exhibit this effect.

The surface charge of ceramics affects tissues and cells. On the negatively charged surface it was noted that the number of osteoblasts increased. They organized themselves and the bone growth occurred rapidly after 1 week implantation. With positively charged surface, the amount of bone formed was the same and it was noted that the cells didn´t show the same arrangement and were disordered [22].

2.3. Adsorption of proteins

The first biomaterials were developed in 1940 and were used for implants, hip joint, dental replacements, eye lens and blood contacting devices [23, 24]. During these discoveries some researchers began studying the surface properties of materials, surface modifications and their interactions. Surface modifications can alter the protein adsorption quantity as well as cell adhesion. There are different methods that permit to modify the material surface. Among them one can mention the application of a surface chemical gradient, self-assembled films, surface-active bulk additive, surface chemical reaction or techniques of material preparation [25].

Surface concepts have been applied in medical and biological technology. Some examples of surface technology applied to biological problems are implant biomaterials, surface diagnostics, laser applications and biosensors. Surface technology is important because it controls biological reactions [26-29].

The adsorption of proteins onto the biomaterial surface or biological tissue is the first process that occurs during the contact between the material and biological fluids (blood or lymph). This process predetermines subsequent body responses [30].

The concept of the tissue engineering resumes to the regeneration or repairing of the tissues [31]. For tissue engineering the adsorption process of proteins is a very important one [32]. During the adsorption process interactions between adsorbed proteins and cells play a key role. Biomaterial substrates can adsorb protein as well as cells, so the competition to be adsorbed does not end [23, 33].

It is important to notice that, together with the surface characteristics of material, the medium also plays a significant role in the adsorption process [34, 35]. Chemical, structural and biological surface properties, their transference into the biological environment, as well as responses, are not sufficiently studied and need further research.

A biological medium includes several types of proteins that can compete for the adsorption process by a specific substrate.

The process of variation of the adsorbed protein layer is shown in Figure 1.3. Different types of proteins according to the bonding force are distinguished in the figure with different colors: red, green or blue [23]. Initially the surface is covered with the layer of red and green adsorbed proteins. The amount and type of adsorbed proteins on the film changes with the time. For example, at t=1 the red and green proteins are the ones preferentially adsorbed, but as time evolves almost all proteins are substituted by blue ones. The substitution is probably associated with the type of bonding protein/material.

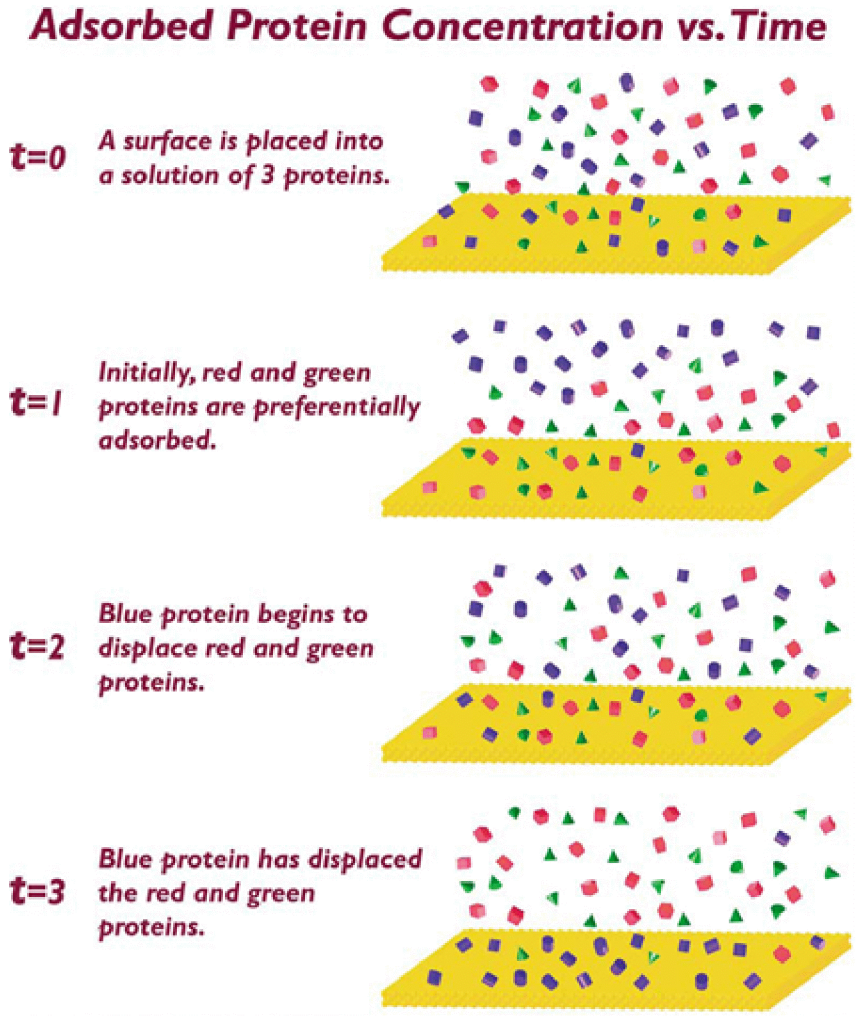

Figure 1.3: The variation of the adsorbed protein layer [23].

Absorbed protein on the surface of a substrate is not stable. Dynamic steps such as desorption, readsorption, conformation or orientation changes are present during the process of adsorption (see Figure 1.4) [34].

Factors such as time and concentration of protein may or not change the conformation or structure of adsorbed protein. Also the type of surface and topography strongly influence the quantity or strength of the adsorbed protein bonding [23].

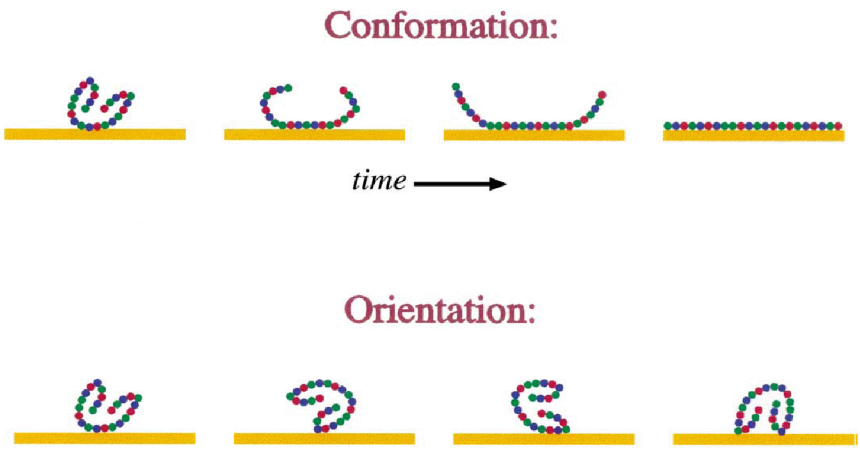

Figure 1.4: The conformation and orientation of adsorbed proteins. The top schematic shows a protein denaturing with increasing adsorption time. The bottom schematic shows a protein adsorbing to the surface in different orientations [23].

2.3.1. Factors that influence protein adsorption

The process of adsorption as a whole is influenced by the rate of protein adsorption, the rate of transport and the rate of unfolding [36, 37].

There are three main types of interactions that are involved in protein adsorption process: hydrophobic, hydrogen-bond and electrostatic [38, 39]. There are different opinions about the type of interaction that mostly affects this process [40]. Some authors defend that hydrophobicity is the dominant in the adsorption process, while others stand for hydrogen-bonding interaction.

According to Ying *et al.* [41] the preferential adsorption of protein occurs on the hydrophobic surfaces (hydrophobic interaction). On the less hydrophobic surfaces the process of protein adsorption is made through the hydrogen bond or electrostatic interaction.

Recently it was discovered that the electrostatic contribution also has an important role among these interactions [41]. Yoon *et al.* [40] has found that an increase of electrostatic groups causes the increase of the amount of adsorbed protein.

The process of protein adsorption is very complex. The main difficulty of understanding this process consists in the fact that most proteins are hydrophilic and hydrophobic at the same time. This can produce different conformations of the adsorbed proteins and also structural changes due to the large contact area of the protein [42].

As mentioned before, other factors may also influence the dynamic process of adsorption such as temperature, pH, time of adsorption and also wettability [43].

Wetting phenomenon is defined by the ability of a liquid substance to form the interaction with a solid surface [44]. Characteristics such as surface chemistry, surface topography and surface thermodynamics can influence the parameters of the surface [45]. The nature of adsorption of proteins onto the surface of materials is also dependent on these parameters.

The formation of the protein layer, size, type of the protein and its ability of adsorption onto the surface of the material can change the chemical, physical and sometimes mechanical properties of the substrate [46, 47]. Surface charge of the biosubstrate, pH, fluid phase composition, chemical composition, temperature and time of contact with protein are factors that influence the composition of the adsorbed protein layer [34]. Table 1 represents the factors that influence the protein adsorption and the respective aspects that are influenced by the factors.

Table 1: Resume of the factors and their influence in the protein adsorption process.

Factors	Aspects
Surface charge a.) Substrate and protein charges are of the opposite sign b.) Substrate and protein charges have the same sign	 increase of the quantity of the protein adsorbed decrease of the quantity of the protein adsorbed
pH	stability of the colloidal suspension and surface charge
Fluid phase	stability of the colloidal suspension, pH and surface charge
Chemical composition	stability of the colloidal suspension and surface charge
Temperature	solubility of the colloid
Time of imersion	qyantity o adsorbed protein

Several works [48, 49] report studies on the relationship between protein adsorption and factors such as hydrophobicity, surface tension and surface charge of materials.

2.3.2. Albumin

Albumin (Fig 1.5) is the most abundant protein in the human plasma (concentration of 38-50 $g.L^{-1}$) with the next chemical formula $C_{2936}H_{4624}N_{786}O_{889}S_{41}$ [50], exerting 75 to 80% of the normal colloid osmotic pressure. This protein has a weight of about 66-kDa. The average particle size of albumin (D_a) is 4.52 nm [51].

Albumin has specific biological function revealed in antioxidant and anti-inflammatory properties [52].

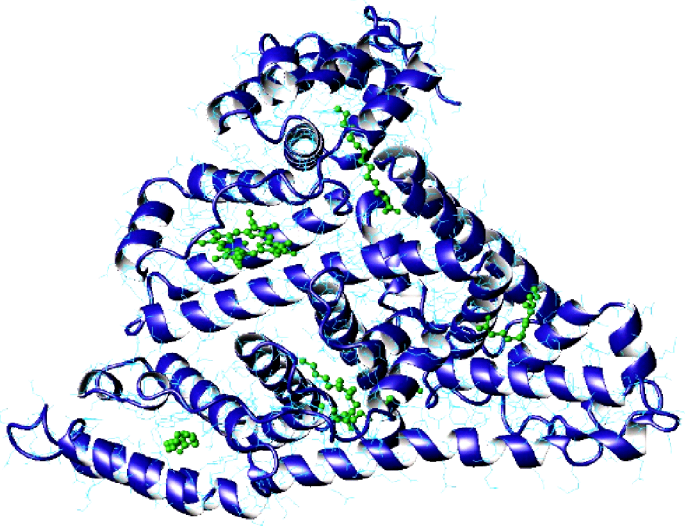

Figure 1.5: Albumin monomer [53]

Albumin can regulate the fluid distribution, binding and transporting of ligands including steroids, fatty acids, bile pigments, metal ions, nitric oxide and drugs. Albumin has a great role in modulating some ligands in blood and phospholipids produced by tumor cells [54].

The charge of albumin is not uniform. Peters *et al.* [55] did experimental work at neutral pH for bovine serum albumin and representation of surface charge distribution is illustrated in Figure 1.6.

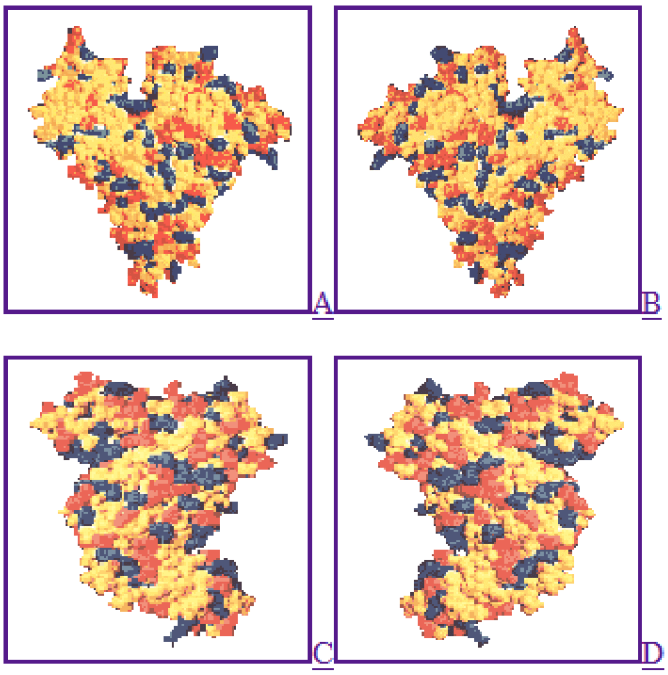

Figure 1.6: The model of serum albumin molecule with basic residues colored in blue, acidic residues in red and neutral ones in yellow. (A) Front view, (B) back view, (C) left side, and (D) right side [55, 56].

In laboratory practice it is important to preserve conservation conditions of BSA. Specific criteria of transport by air should be accounted for. A lot of modifications and dysfunctions may be provoked by the contact with metabolites, toxins or drugs [57].

BSA was chosen to conduct the experimental work further described in section 4 due to its relatively low cost, availability, solubility in aqueous medium and homogeneity. This protein will be used during a series of repeated experiments aimed to compare its adsorption behavior onto different materials under different conditions.

2.4. Surface Charge and Zeta Potential

It is well accepted the importance of the surface properties of materials and its relation with biological responses when implanted [58]. Among these properties one can mention the surface chemistry, charge and the surface topography [59]. The surface chemical compositions of substrates also have a strong effect on the protein adsorption process.

Zeta potential is used to determine the stability of colloidal suspensions, where the solid is suspended in a liquid. It is known that colloids with high zeta potential (negative or positive) are electrically stable while colloids with low zeta potentials tend to coagulate or flocculate as presented in Table 2 [60].

Table 2: Stability behavior of colloids related with value of zeta potential [60].

Zeta potential (mV)	Stability behavior of the colloid
from 0 to ±5	Rapid coagulation or flocculation
from ±10 to ±30	Incipient instability
from ±30 to ±40	Moderate stability
from ±40 to ±60	Good stability
more than ±61	Excellent stability

2.4.1. Zeta potential fundamental concepts

The double layer model is forward to explain the distribution of ions around the particle. Counter ions that attach to a charged surface form the Stern layer. Ions that concentration decreases by increasing the distance from the surface of substrate form the Diffuse layer. The result of a zeta-potential measurement is the potential at the boundary between the Stern layer and the Diffuse layer (Figure 1.7). It is based on the charge displacement in the electric double layer that is caused by the potential difference between the liquid and the solid phases [58].

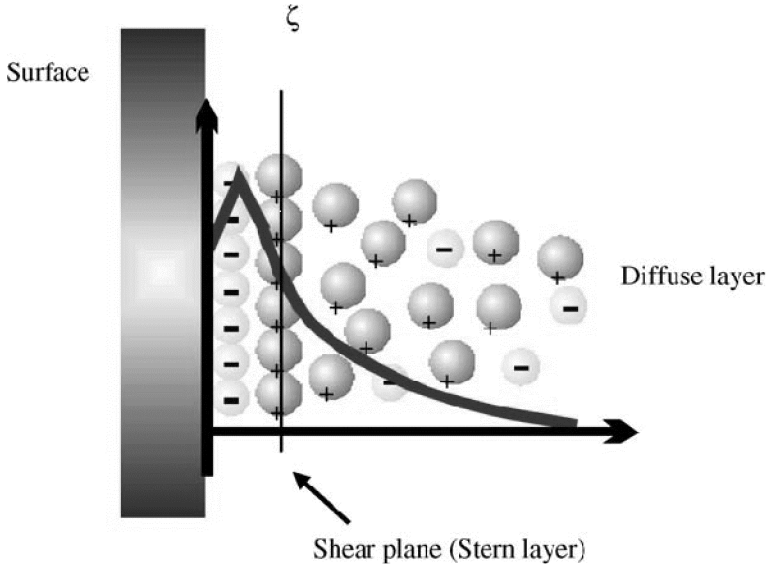

Figure 1.7: Schematic diagram of the electric double layer in zeta-potential measurement [58].

Figure 1.7 shows that the concentration of ions decreases from the Stern layer to the Diffuse layer [61, 62]. The isoelectric point (IEP) is an important parameter that demonstrates the exact pH value at which the surface of the particle obtains zero charge [63].

There are different methods used to measure the zeta-potential. The most widely used is electrophoresis and it is based on the theory of Smoluchowski that proposed that the velocity of particles motion in the electric field is proportional to the zeta potential [62]. This theory of electrophoresis can be interpreted by the equation 1 [64].

$$\mu_e = \frac{\varepsilon_r \varepsilon_0 \zeta}{\eta} \qquad \text{eq. 1}$$

where ε_r stands for the dielectric constant of the dispersion medium, ε_0 for the permittivity of free space ($C^2\ N^{-1}\ m^{-2}$), η for the dynamic viscosity of the dispersion medium (Pa.s), and ζ for the zeta potential.

In some applications zeta potential is measured to determine the magnitude of the potential of the particles [65]. For example it is used to obtain the charge of the particles in aggregation behavior, flow, sedimentation, and filtration.

Variation of pH can be obtained by the addition of acids or bases, such as HCl or KOH, respectively. Tassel *et al.* [66] found a relationship between the quantity of reagents (HCl and KOH used to establish the desired pH) and zeta potential (Figure 1.8). The addition of KOH reagent provokes the decrease of the zeta potential value from positive to negative one. This phenomenon is not occurring after addition of HCl reagent, the zeta potential doesn't decrease to negative values.

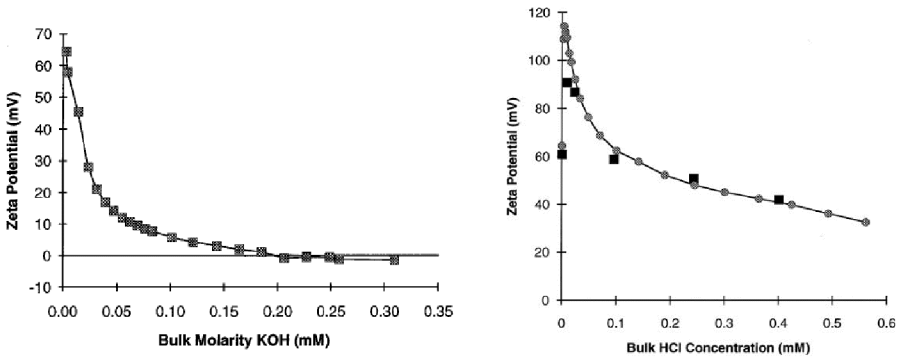

Figure 1.8: Zeta potential as a function of molarity of KOH and HCl respectively in ethanol/water solution [66].

The zeta potential is affected by the particle size of the substrate [63, 67]. Concerning biomaterials particles there is not a systematic study of the variables

that affect the zeta potencial, but these relationships have been studied for other materials.

Figure 1.9 represents the relationship between zeta potential and the particle size at a given pH [63] for kaolin.

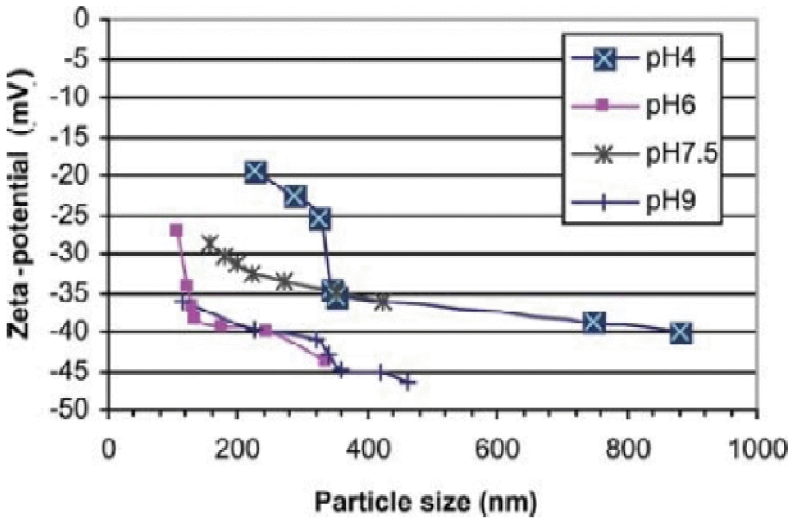

Figure 1.9: Comparison of zeta potential and particle size of kaolin at pH 4, 6, 7,5 and 9 [63].

It is observed that the decrease of particle size is accompanied by an, increase of the zeta potential.

2.4.2. In vivo zeta potential phenomenon

In contact with aqueous medium in vivo bone creates surface charge. The difference in charge between the solid phase of bone and the liquid one creates a potential difference between these two phases associated with the concept of zeta potential (ζ), which determines the nature of the surface charge [61, 62].

Both the organic and the mineral part of the bone can create a zeta potential but the determinant one is the organic part – the collagen. This fact was studied by Otter *et al.* [68], in 1988. The experimental work has shown that the zeta potential of hydroxyapatite (mineral component of bone) is much smaller than the one of the collagen. One of the possible reasons that could explain this phenomenon is that the HA surface contains HPO_4^{2-} and $H_2PO_4^-$ ions that turn this surface more negative than of the collagen. It was concluded that the organic part is a major contributor to the zeta potential, and variation of the piezoelectricity of the bone [12].

Factors such as the chemical composition, the inflammatory situation, the composition of the surrounding solution and the pH value influence the electrical charge of the material surface [61]. The relationship between the surface chemistry, electric charge on a surface and protein adsorption is very important for the understanding of the complexity of biological processes related with tissues. This knowledge can be used to the improvement of the quality of the implants and biomedical devices.

3. The selected materials

In the present work three different materials were selected for the adsorption studies with BSA: hydroxyapatite, a glass with *in vitro* bioactivity developed in our laboratory (V7) and poly-L- lactide acid (PLLA). The three are briefly presented in the next sections.

3.1. Hydroxyapatite

Hydroxyapatite ($Ca_5 (PO_4)_3 (OH)$) is the major inorganic constituent of bone (~70%). In a synthetic form it is largely used for bones and teeth implants as well as for a lot of other medical and biomedical applications. This popularity can be explained by the high biocompatibility and bioactivity of hydroxyapatite (HA) and the possibility that it has to form a strong bond with hard tissues [69].

A factor that gives to hydroxyapatite a good stability and a great number of applications is its good biocompatibility and a molar Ca/P ratio near 1.67. Huang *et al.* [70] found that hydroxyapatite can be composed by nanometer-sized crystals, poor crystallinity and ionic (cationic and anionic) substitutions. Ions have an effect on such factors as crystal size and crystallinity that in their turn affect the stability and solubility of HA, influencing pH of the suspension and the surface charge of the substrate.

It is known that HA is one of the constituents of tooth. The natural formation of enamel is based on a process of proteins adsorption onto tooth surface [71]. This pellicle is very important for the adsorption process of microorganisms. Problems of caries have led to more detailed studies of proteins. It is reported that proteins are the inhibitors of enamel and dentine demineralization and are located between tooth and dental plaque [71].

The process of adsorption of BSA onto HA surface is a complex one that consists in electrostatic attraction between the COOH group of BSA or in ion exchange. Among ions of HA, calcium and phosphate, only the last one is released when acidic proteins are adsorbed [72].

Formation of apatite brings some changes to HA namely in the surface structure, and in the interactions between HA surface and calcium and phosphate ions from Phosphate buffered saline (PBS). Figure 1.10 represents the mechanism of apatite formation on HA when immersed in PBS buffer solution. There are three processes involved in the apatite formation: adsorption of calcium ions (Ca-rich ACP), phosphate ions (Ca-poor ACP) and both the calcium and phosphate ions [73].

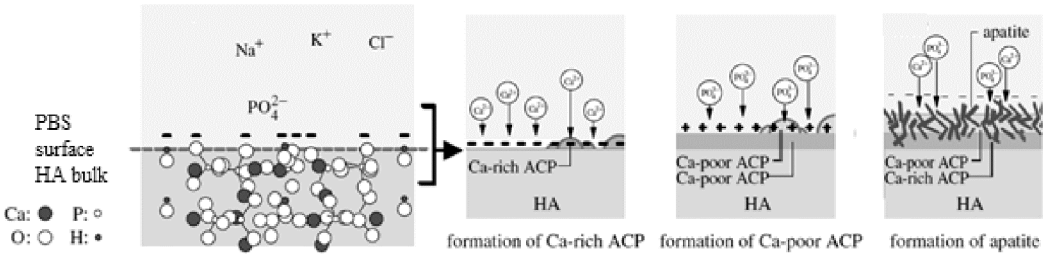

Figure 1.10: Schematic representation of the origin of the negative charge on the HA surface and the process of bone-like apatite formation thereon in PBS (adapted from [74]).

Studies have shown that the increase of the PO_4^{3-} decrease the amount of adsorbed BSA. To separate the adsorbed biological molecules from surfaces these ions can be used [74].

The amount of adsorbed albumin depends on the molar ratio between cations and phosphorus of the used materials [75]. A factor that can influence the adsorbed amount of protein to hydroxyapatite is the material texture and the kind of crystal face exposed at the particle surface, though, there was not found any systematic study on this subject in the literature.

3.2. Bioactive glasses

A bioactive material can form a chemical bond with bone *in vivo* [76]. This ability can be found in materials such as glasses, glass ceramics and calcium phosphates.

Bioactive glasses were first used in 1969 for the bonding of the implant to the host tissues [77]. Grafts for bone repair and regeneration should exhibit several capabilities such as osteogenicity, osteoinductivity and osteoconduction [76]. Bone implants from glasses and glass-ceramics are based on the SiO_2–CaO– P_2O_5 system and have a great number of applications in medicine.

The Bioglass ® discovered by Hench *et al.* [3] is one of the most accessible bioactive materials. Several compositions were developed within the Na_2O-CaO-

P_2O_5-SiO_2 system with a constant percentage of P_2O_5 (6% weight). Different bioactivity behaviors were found, depending on the composition and system [3].

An apatite layer responsible for bioactivity is formed on the surface of bioglasses when they are immersed into solutions that mimick the human blood plasma. Hench [3] proposed a mechanism of apatite formation on the surface of bioglass that consists of five stages, three of which correspond to chemical corrosion that happens to any alkali or alkaline earth glass when immersed in an aqueous solution [78]:

Stage 1: Rapid exchange between alkali ions of the glass and H^+ ions from solution as represented by the chemical equation:

$$Si-O-Na^+ + H^+ + OH^- \rightarrow Si-OH^+ + Na^+ + OH^-$$

Stage 2: Dissolution of the glass network resulting in the breaking of Si-O-Si and formation of Si-OH groups on the glass-solution interface, as represented by the chemical equation:

$$Si-O-Si + H_2O \rightarrow Si-OH + OH-Si$$

Stage 3: Condensation of Si-OH groups and formation of a layer rich in silica gel on the glass surface devoid of alkali ions and alkaline-earth, as represented by the chemical equation:

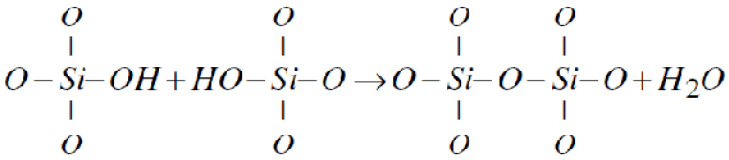

Stage 4: Migration of ions Ca^{2+} and PO_4^{3-} onto the surface layer of silica gel forming an amorphous film rich in CaO-P_2O_5 (Ca-P)

Stage 5: Crystallization of the amorphous film by incorporation of OH^- and CO_3^{2-} anions from the solution

According to Lu *et al.* [78] there is a relationship between surface charge of a bioglass and its biological response. These authors studied the relationship between the variation of the surface charge of bioglasses by measuring the zeta potential, the variation of the concentration of phosphate ions in the buffer solution and the formation of Ca-P layer on its surface when immersed in a physiological fluid. It was observed that the zeta potential of bioglass varied continuously with changes in surface charge of bioglass and depended on the state of the surface composition, structure and morphology. Within the range of pH in the human body it was found that the surface charge is negative, which is in agreement with one of the criteria defined by Li *et al.* [3] for a bioactive biomaterial.

3.3. Poly-L-lactide acid

Poly(L-lactide) (PLLA) is considered an attractive biomaterial because of its biodegradable properties. It is used for many biomedical applications such as sutures and drug delivery devices [79]. This polymer is semicrystalline, biocompatible and bioresorbable [80] and has the chemical composition $C_3H_4O_2$ [81], as schematically shown in Figure 1.11.

The mechanical properties and thermal degradation of PLLA may be varied by the variation of its molecular weight and the content of the crystalline phase [3]. Unfortunately, its toughness at high temperature is not favorable for some practical application. The mixture of PLLA with other polymers creates an economic method to obtain toughened products.

Hydrophobic surface of PLLA can represent strong protein adsorption behavior [81] since proteins usually tend to adsorb onto hydrophobic polymer surfaces rather than onto hydrophilic ones.

Indeed PLLA is one of the few materials that are approved for applications into the human body. This was one of the reasons for the choice of PLLA in this work.

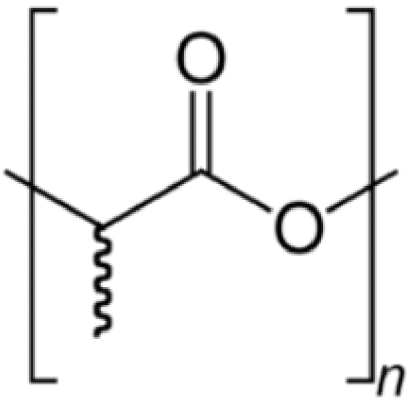

Figure 1.11: Repeating unit of PLLA [82].

4. Materials and methods

This section presents the characterization of the materials selected in this study and also the techniques and methodologies used in the experimental work.

Three materials were used as substrates: HA, bioglass V7 and PLLA. After the preparation or milling treatments all the materials were submitted to a granulometric analysis to assess the particle size distribution.

XRD was performed on all materials in order to determine the crystalline phases present or to confirm the amorphous nature of the powders.

The morphology and size of the particles was observed by Scanning Electron Microscopy (SEM).

Bovine Serum Albumin (BSA) was the protein chosen to evaluate the effect of the surface charge of these materials on protein adsorption.

All suspensions and solutions were made in a Phosphate Buffered Saline (PBS) medium.

A summary of the relevant characteristics of the materials used in the experiments (solids or liquids) is presented in the following sections.

4.1. Materials characterization

Hydroxyapatite

The hydroxyapatite powder used in this work was provided by the CAPITA®S company. The particle size distribution (Figure 2.1) obtained by Coulter Counter LS 230 shows that the average size (D_a) of the particles is 1.8 µm.

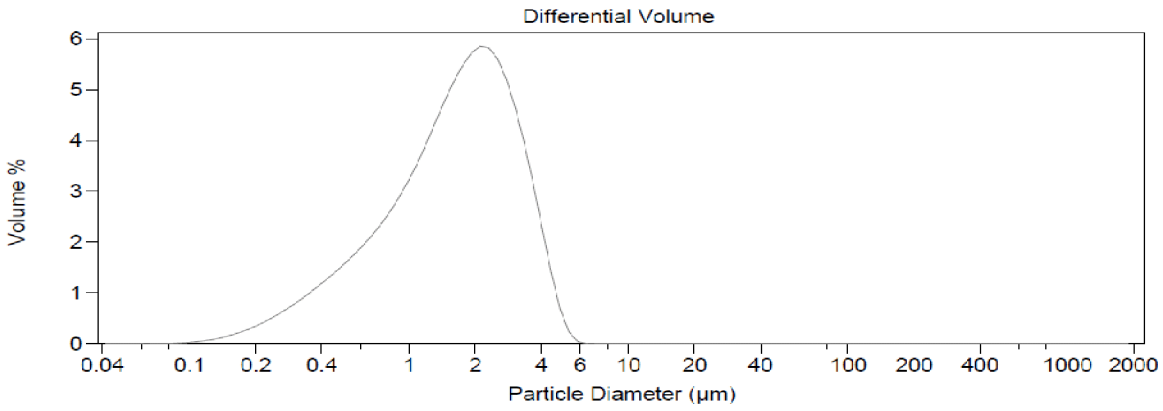

Figure 2.1: Particle size distribution of HA powders

SEM micrograph of HA particles (Figure 2.2) confirmed the size distribution results, with particles not exceeding 6μm.

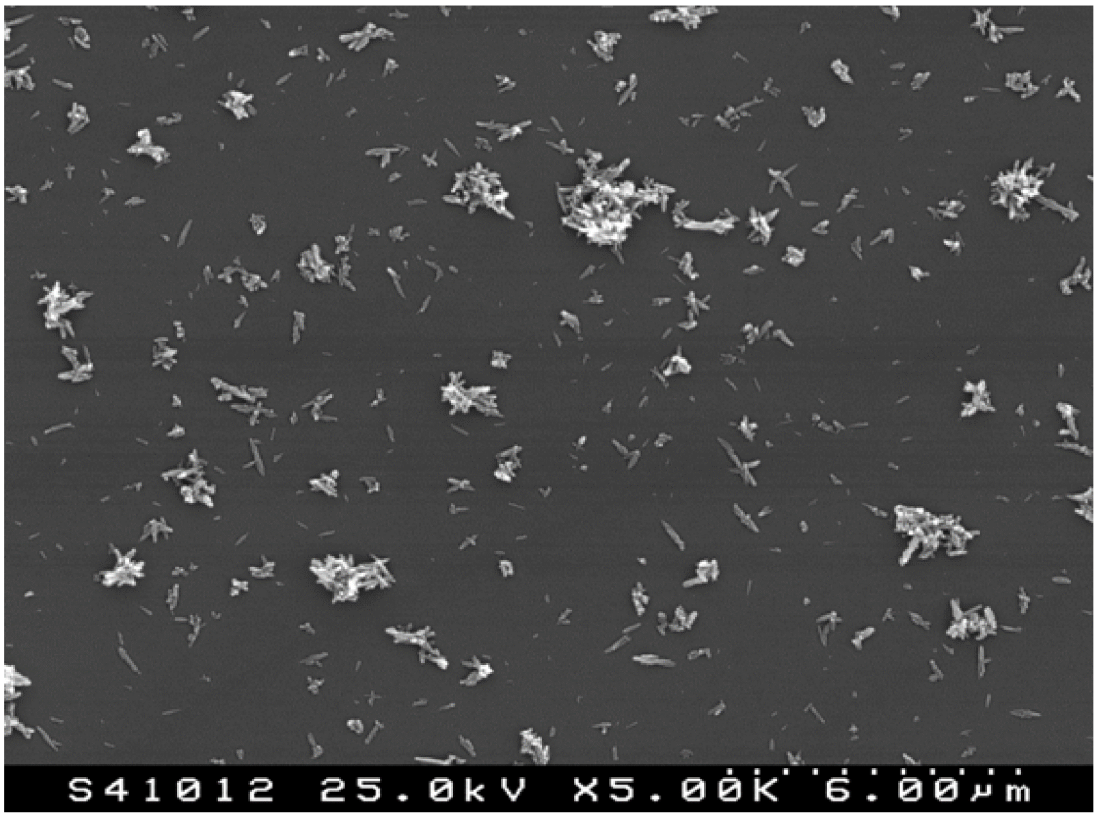

Figure 2.2: SEM micrograph of HA particles

The XRD patterns of HA powders are illustrated in Figure 2.3.

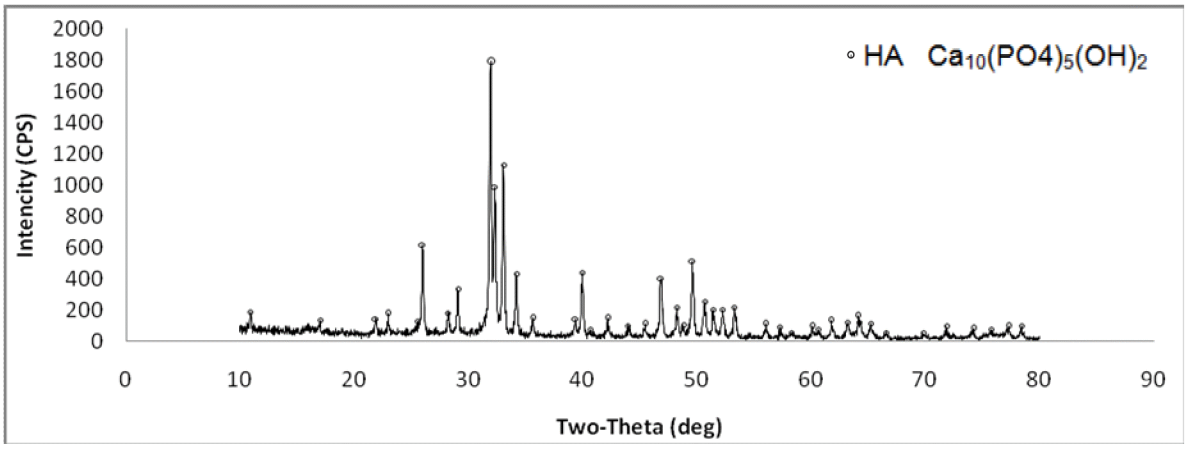

Figure 2.3: XRD of HA

The Specific Surface Area (SSA) of HA particles was 8.9 m²/g, as measured by the Brunauer, Emmett and Teller technique (BET).

Bioglass V7

The selected bioglass, V7, was developed by the group at the University of Aveiro, belongs to the system $3CaO.P_2O_5.MgO.SiO_2$ and has a composition (wt%) of $33.2CaO.28.2P_2O_5.15.6MgO.23.0SiO_2$ (Figure 2.4). This glass exhibited a bioactive character in physiological synthetic acellular medium and showed to be able to induce the proliferation of MG 63 osteoblast-like cells [3]

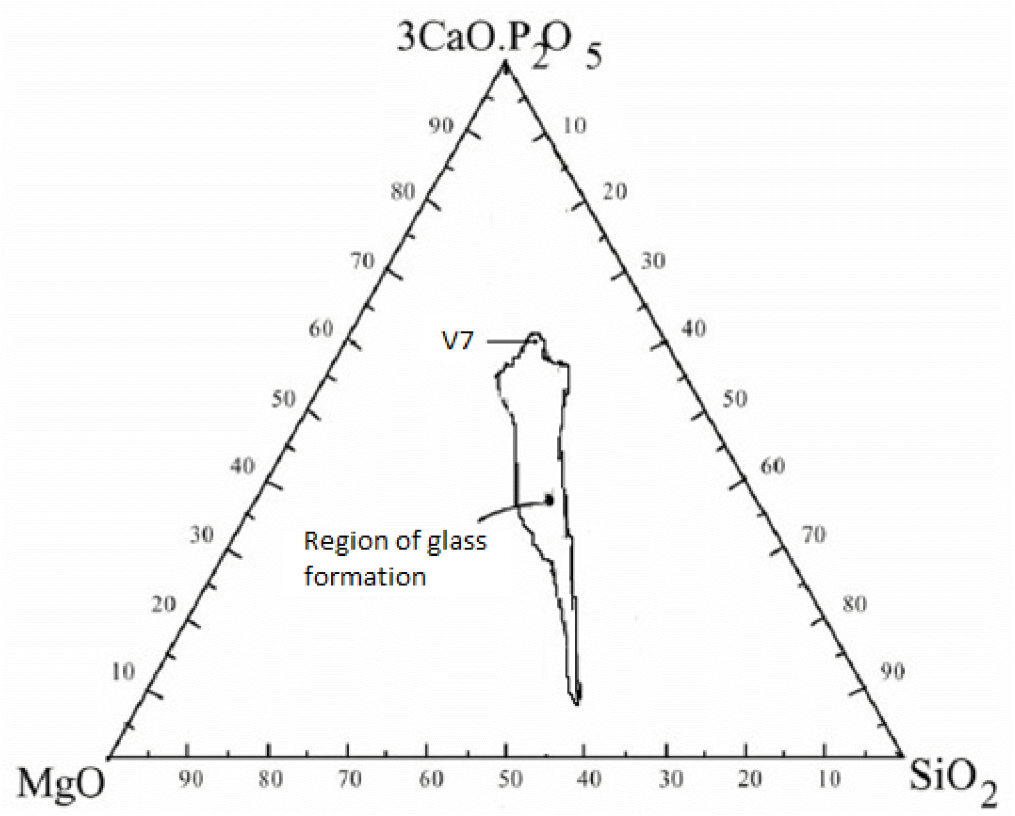

Figure 2.4: Ternary diagram of the system 3CaO.P2O5-SiO2-MgO (wt%) with reference to the bioglass V7 (Adapted from [3]).

Bioglass V7 was prepared from the raw materials: SiO_2 (Merck), MgO (Fluka), $CaCO_3$ (Fluka), and $CaH_4O_8P_2H_2O$ (Fluka). Powders were milled in a planetary ball mill (Fritsch) for 45 min with alcohol the desired particle size was obtained. After milling the product was dried at 75ºC for about one day.

The batch was melted at 1500ºC for 1 hour and the melt was poured to a water reservoir to obtain a frit. The glass frit was dried at 75ºC during 20 hours.

According to the requirement of Zetasizer device, to provide the correct measurement of the zeta potential, all powders must have size between 0.6 nm and 6 µm. To obtain the granulometric distribution shown in Figure 2.5 the bioglass was dry milled for 8h and then wet milled with ethanol for 3h and 30min. The granulometric analysis of bioglass V7 has shown that the average size of the particles is 2.73 µm.

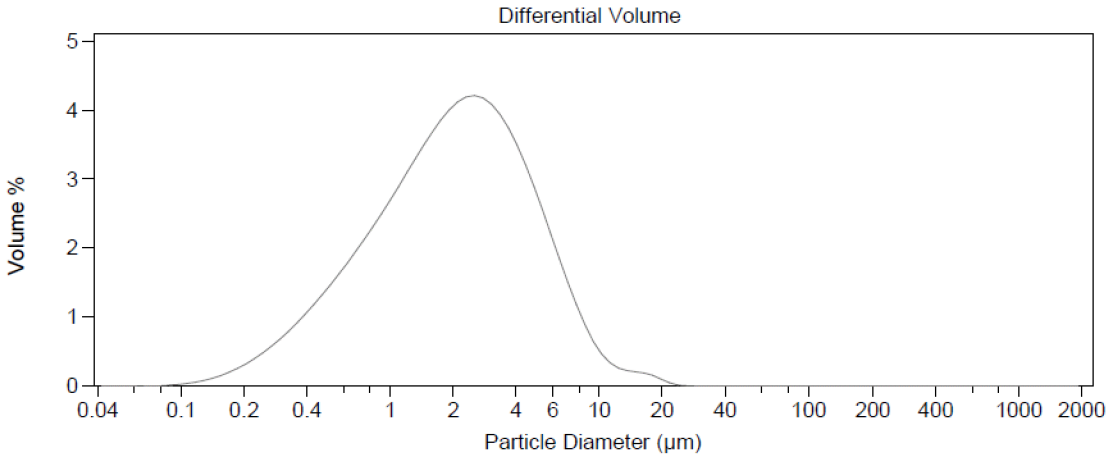

Figure 2.5: Granulometric distribution of bioglass V7 powder.

SEM micrograph of bioglass V7 particles is shown in Figure 2.6

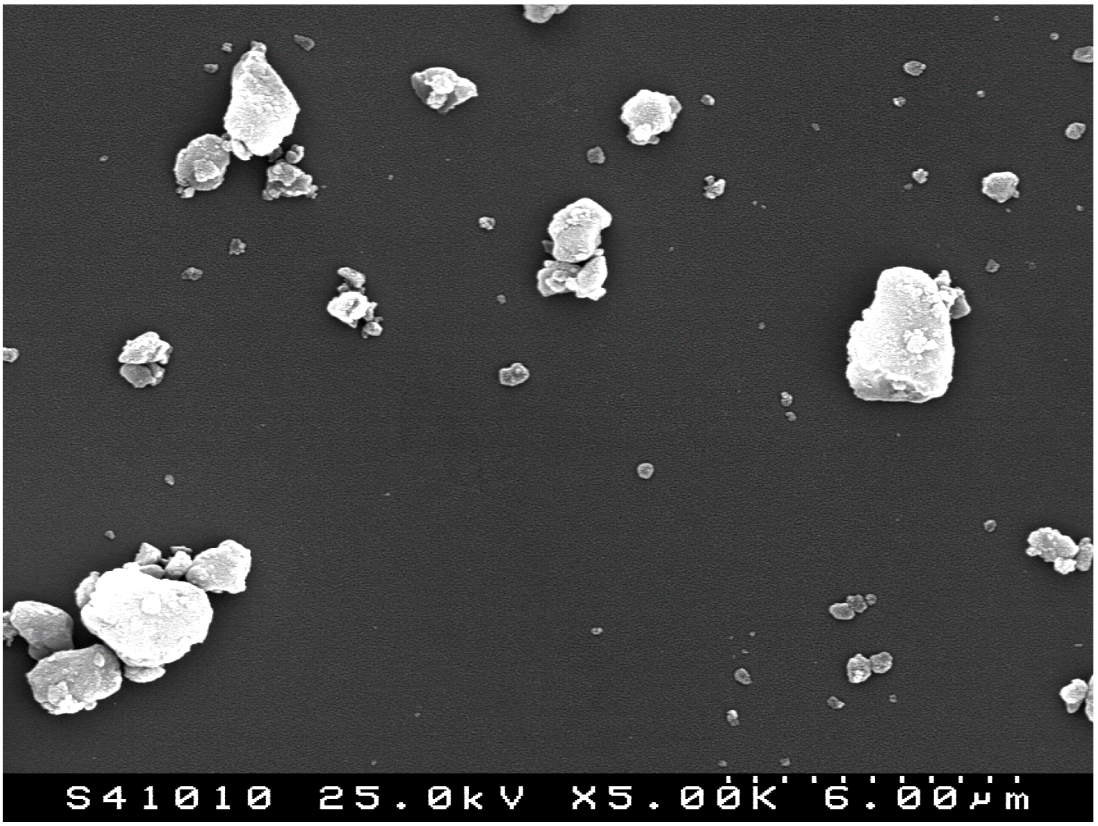

Figure 2.6: SEM micrograph of bioglass V7 particles

XRD to the bioglass V7 confirmed its amorphous nature as shown in Figure 2.7.

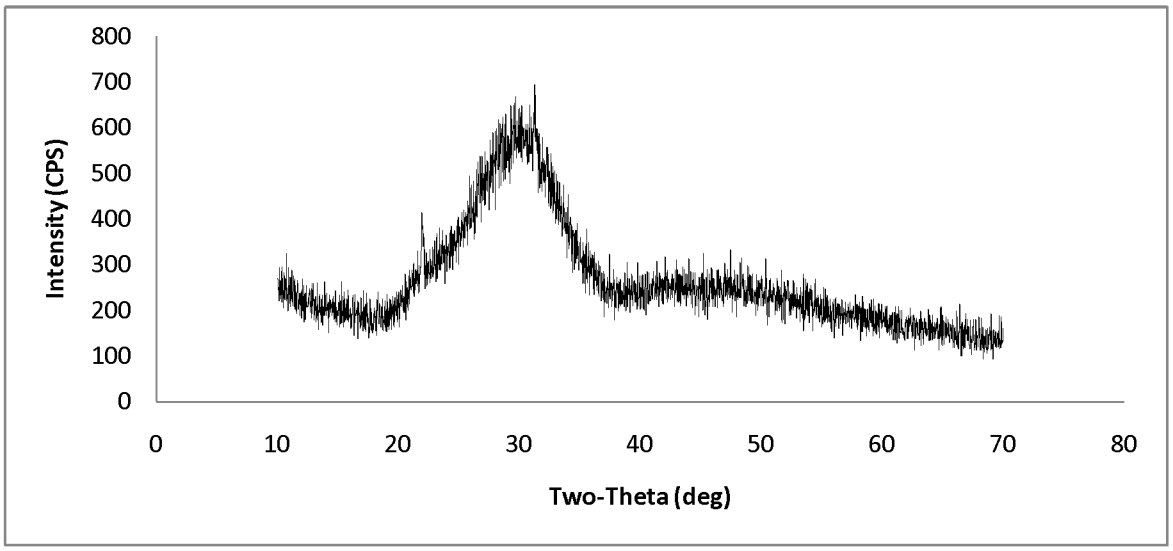

Figure 2.7: XRD pattern of bioglass V7.

BET method indicated a value of 1.8 m²/g for the SSA of V7 particles.

PLLA

PLLA powder used in the experimental work was produced by PURAC Biochem bv Gorinchem in Holland. It was stored in a closed package in a freezer and put at room temperature before opened.

After submitted to dry milling the average size of the particles is 4.68 µm (Figure 2.8).

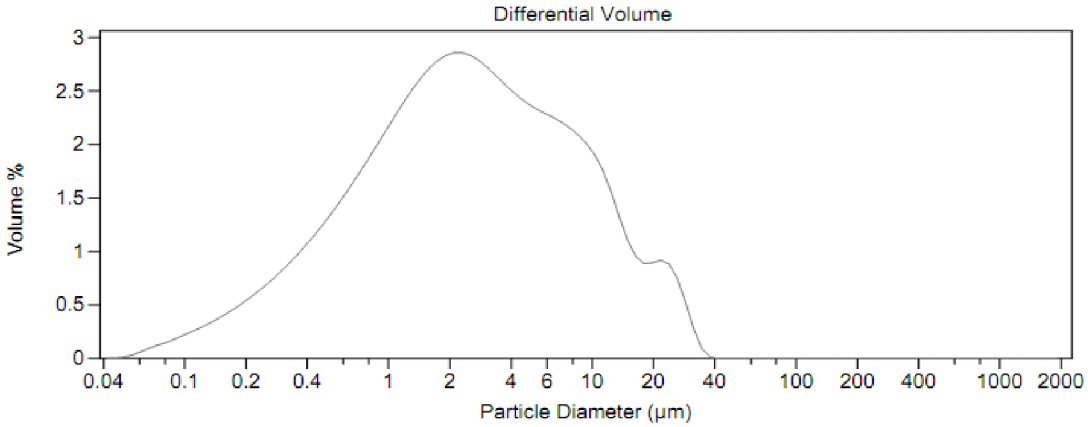

Figure 2.8: Granulometric distribution of PLLA.

SEM observation of PLLA particles confirmed the granulometric distribution results (Figure 2.9).

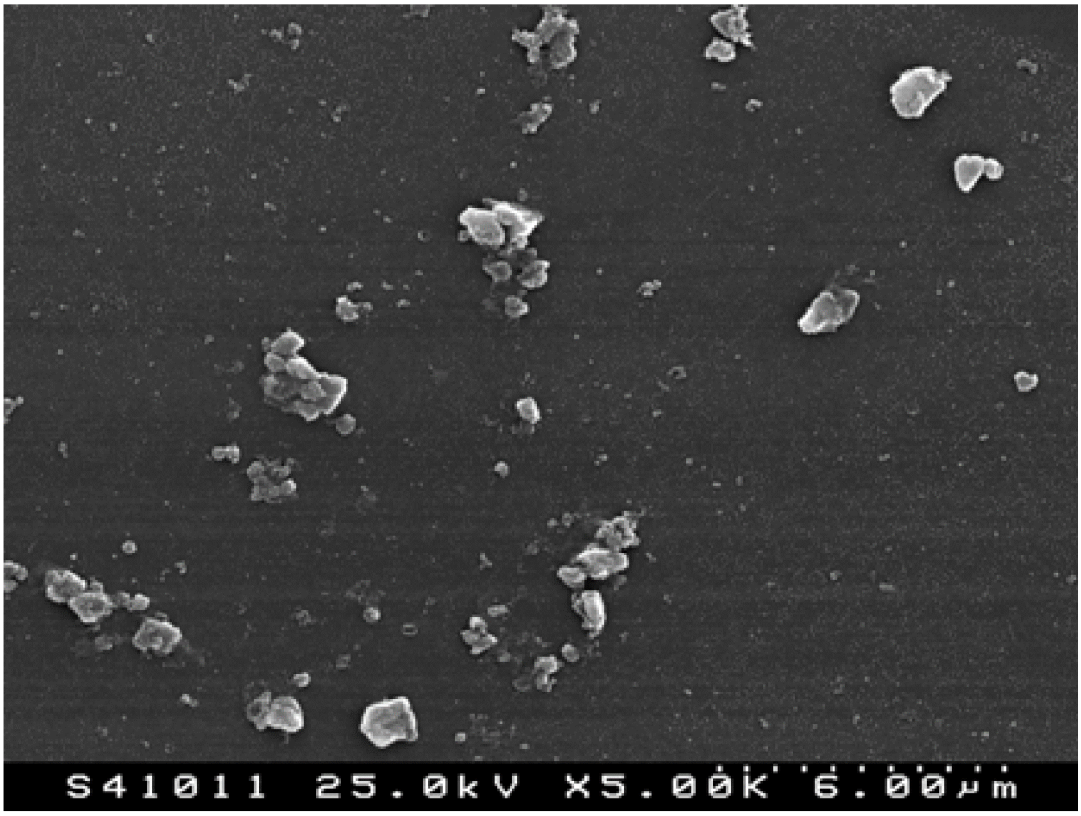

Figure 2.9: SEM micrograph of PLLA particles

Figure 2.10 shows the XRD pattern of PLLA

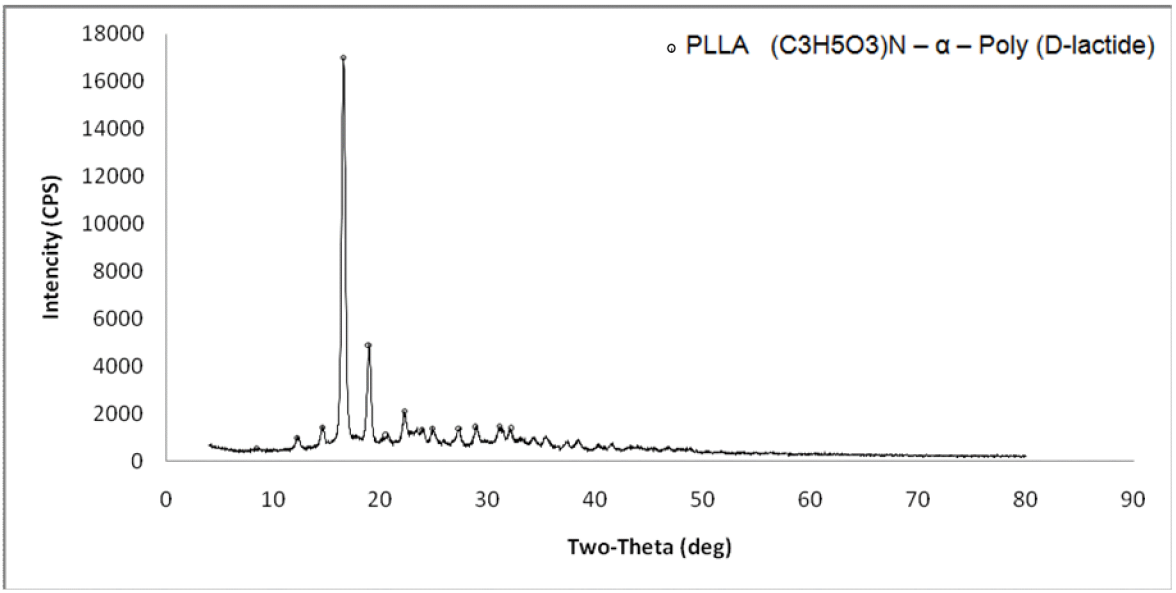

Figure 2.10: XRD pattern of PLLA.

The SSA by BET method is 18.71m²/g for PLLA particles.

Phosphate buffered saline (PBS) solution

Phosphate buffered saline is a buffer solution largely used in *in vitro* experiments in the biological area [83] due to the non toxic composition and to the similarity to human plasma.

One of the most common compositions of PBS is presented in Table 3.

Table 3: One of the common compositions of PBS [84]

Salt	Concentration	Concentration
(-)	(mmol/L)	(g/L)
NaCl	137	8.00
KCl	2.7	0.20
Na2HPO4	10	1.44
KH2PO4	1.76	0.24
pH	7.4	7.4

The PBS P-3813 used in the present experimental work was produced by SIGMA company [85]. PBS was used in the form of dry powders. The powders were dissolved in 1 liter of deionized water (pH 7.4 at 25ºC) to obtain 0.01M PBS.

Albumin

To simulate human albumin it was used a bovine serum albumin, BSA, (Serva 11930, lot nº. 15538) with pH 7.0. BSA has the advantage of being cheaper than human albumin and is very similar to it in the sequence of amino acid units. The BSA powder was dissolved in PBS solution.

4.2. Methods and Methodologies

Surface charge of the several materials (HA, bioglass V7 and PLLA) was assessed by zeta potential measurements performed with a Zetasizer Nano series equipment. This apparatus calculates the zeta potential by determining electrophoretic mobility and then applies Henry equation (equation 2) [86].

$$p = kc \qquad \text{eq.2}$$

where p stands for the partial pressure of the solute, c for the concentration of the solute in the solution and k ($Pa \cdot m^3/mol$) for the Henry's Law constant [87].

Suspensions for the zeta potential measurements were prepared by adding 3 mg of the substrate particles to 15 ml of PBS to obtain a concentration of 0.2 g/l. Some experiments were carried out with suspensions of the particles in water. The pH of the suspensions was adjusted by using NaOH or HCl to increase the alkalinity or the acidity, respectively.

To determine the differences of protein adsorption onto the several materials, the different suspensions of PBS + powders were added with 0.33 g/L of BSA and kept at 36 ºC for different times. The quantification of BSA adsorbed was made by the Lowry method described later in this section.

To understand how protein adsorption can change along the time due to the gradual surface enrichment of protein, zeta potential measurements were also performed on powders previously put in contact with albumin.

A summary of the different experimental conditions for the zeta potential measurements is presented in Table 4a for HA, Table 4b for bioglass V7 and Table 4c for PLLA. Each group of data (from A to L) represented in the table corresponds to a series of experiments carried out under the required conditions. More details are shown in Annex 1.

With exception of the experiments carried out with variable time, all the zeta potential measurements were performed after incubation (kept at required conditions) of materials for 24 hours at the conditions described.

Table 4a: Experimental conditions for zeta potential measurements for HA in PBS (T=36ºC; D_a = 1.81 µm)

	Parameter	Experiments			
		Group A	Group B	Group C	Group D
HA	pH	2.75-11.72	2.57-12	7.7	7.7
	t (h)	24	24	24-272	100
	BSA conc in PBS (g/L)	0	0.33	0.33	0.06-2.26

Measurements in water were carried out in the range of pH 2.33-11.2 after 24h of incubation. Zeta potential measurements were also performed in water at 25ºC, after 24h of incubation in the range of pH 2.53-11.43.

Table 4b: Experimental conditions for zeta potential measurements for bioglass V7 in PBS (T=36ºC; D_a = 2.73 µm)

	Parameter	Experiments			
		Group E	Group F	Group G	Group H
Bioglass V7	pH	2.85-11.6	2.39-11.27	7.7	7.7
	t (h)	24	24	24-240	100
	BSA conc in PBS (g/L)	0	0.33	0.33	0.12-2.97

Table 4c: Experimental conditions for zeta potential measurements for PLLA in PBS (T=36ºC; D_a = 4.68 µm)

	Parameter	Experiments			
		Group I	Group J	Group K	Group L
PLLA	pH	2.33-11.16	2.41-11.26	7.7	7.7
	t (h)	24	24	24-240	100
	BSA conc in PBS (g/L)	0	0.33	0.33	0.087-3.26

BSA quantification by the Lowry method

The Lowry method is a standard method for protein quantification [88] and a modified Biuret Reaction, more sensitive than this one that uses Folin-Ciocalteu reagent for color identification [89].

In the Lowry method the –CO–NH– (peptide bond) reacts with copper sulfate in alkaline medium to give a complex with some protein residues like tyrosine and tryptophan [90]. The color reaction in the Lowry procedure occurs when the tetradentate copper complexes transfer electrons to the phospho-molybdic acid complex [89].

The Lowry method is sensitive to pH changes and therefore the pH of assay solution should be kept between 10 and 10.5. This method has the great advantage of its sensitivity to low concentrations of protein (up to 0.005 mg/ml [90]). The main drawback is the instability of alkaline copper reagent used in the method. In addition, during the experimental work it is necessary to have the same level of illumination.

The reagents used to the albumin quantification process are not specified because they have protected compositions and are designated as reagent A, reagent B and reagent C. These reagents can be used with 10% SDS (sodium dodecyl sulfate), the detergent employed in the Lowry method.

The process of albumin quantification followed the steps indicated below:

1. Centrifugation of the sample.
2. Removal the supernatant from the sample.
3. Washing of the material to remove the albumin released from the surface and confirm the absence of BSA by UV spectrometer Shimadzu UV-3100.(absence of BSA was obtained after 3 washes)
4. Addition of 300µl of SDS 10% solution to remove the BSA from the surface of material.
5. Centrifugation of the sample.
6. Removal of the supernatant from the sample.

This process was followed by the next protocol to quantify the BSA:

1. Addition of 20µl of reagent C to 1ml of reagent A to obtain A'.
2. Preparation of standard solutions of BSA between 0.2 mg / ml to 1.5 mg / ml (it may be prepared in the same buffer of the sample) to obtain the calibration line.
3. Pipette 10µl of sample to the microtubes.
4. Addition of 50µl of reagent A' to each microtube of the sample.
5. Addition of 400µl of reagent B (contains copper and will react with the peptide bond) to each microtube and incubate at room temperature for 15 minutes.
6. Measurement of the peak of absorbance of each sample with UV spectrometer.
7. Use of the calibration line for each of the previously obtained results to measure the BSA value in µg.

To convert the BSA values to µg/m² the next formula was used (eq. 3):

$$W_T = \frac{m_{BSA}}{m_s \times A} \qquad \text{eq. 3}$$

where W_T stands for the BSA weight per area in µg/m², m_{BSA} for the mass of adsorbed BSA in µg, m_s for the mass of the substrate in g and A is the BET surface area in m²/g.

Quantification of BSA adsorption onto the different materials was performed for different experimental conditions to assess the influence of a) pH of suspension, b) incubation time and c) BSA concentration.

A summary of the different experimental conditions for the BSA quantification is presented in Table 5a for HA, Table 5b for bioglass V7 and Table 5c for PLLA. More details are shown in Annex 2.

Table 5a: Experimental conditions for BSA quantification for HA in PBS (T=36ºC; D_a = 1.81 µm)

	Parameter	Experiments		
		Group A	Group B	Group C
HA	pH	2.93-10.64	7.6	7.6
	t (h)	24	24	24 and 168
	BSA conc in PBS (g/L)	0.33	0.1-1	0.33

Table 5b: Experimental conditions for BSA quantification for bioglass V7 in PBS (T=36ºC; D_a = 2.73 µm)

	Parameter	Experiments		
		Group D	Group E	Group F
Bioglass V7	pH	3.11-11.01	7.7	7.7
	t (h)	24	24	24 and 168
	BSA conc in PBS (g/L)	0.33	0.1-1	0.33

Table 5c: Experimental conditions for BSA quantification for PLLA in PBS (T=36ºC; D_a = 4.68 µm)

	Parameter	Experiments		
		Group G	Group H	Group I
PLLA	pH	2.73-10.87	7.7	7.7
	t (h)	24	24	24 and 168
	BSA conc in PBS (g/L)	0.33	0.1-1	0.33

5. Results and Discussion

In this section we will discuss the results obtained in the experimental work described in the previous section and conducted with the objective of studying the effect of the surface charge of different substrates on the quantity of BSA adsorbed onto the surface of those substrates.

Surface charge was assessed by zeta potential measurements and BSA was quantified by the Lowry method. Different experiments were conducted during which the medium conditions such as pH, immersion time of the substrate and BSA concentration were altered.

5.1. Zeta potential as a function of pH

The variation of the surface charge with pH can be schematically represented in Figure 3.1 [91]. With the increase of pH the surface charge of the substrate becomes more negatively charged. For low pH values the surface is positively charged.

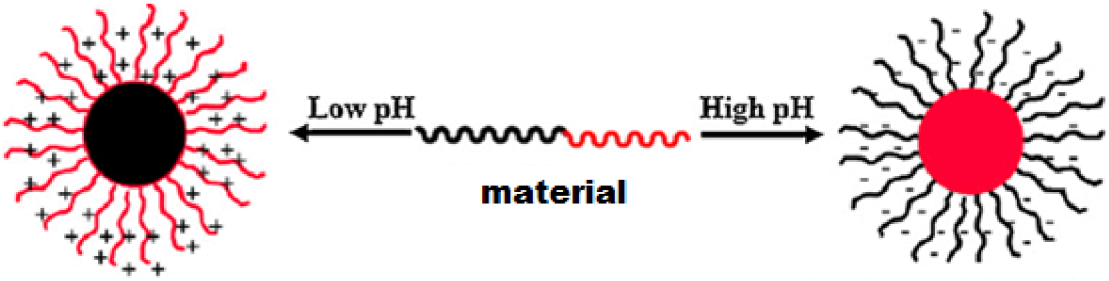

Figure 3.1: Representation of the variation of the surface charge of material at low and high pH (adapted from [98]).

Experiments with BSA

Figure 3.2 represents the variation of BSA zeta potential as a function of pH being the experiments carried out at 36ºC in PBS with the addition of 2g/L of albumin.

For low pH values the zeta potential of BSA is positive. As the pH increases the zeta potential decreases and the isoelectric point (IEP) is found for pH=4.7. For further increase of pH the zeta potential decreases followed by an increase

after pH = 7.5. The phenomenon that occurs between pH 7.5 and 9.5 is probably due to the adsorption of counter ions that make the surface charge more positive and produce the observed inflection in the zeta potential trend.

The literature reports that the value of IEP of BSA varies from 4.6 to 4.9 [92], but the variation of zeta potential with pH is not referred.

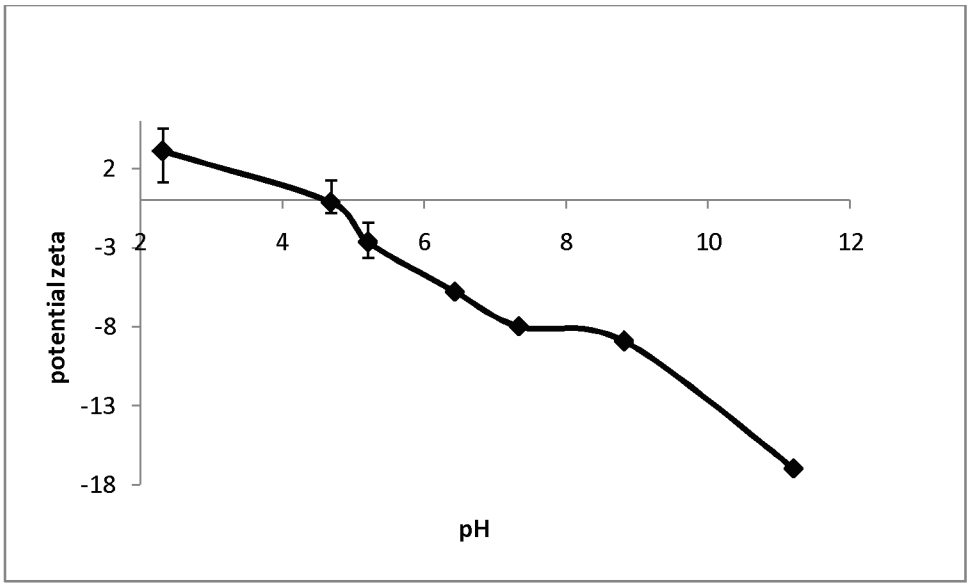

Figure 3.2: Variation of BSA zeta potential as a function of pH

Bovine Serum Albumin (BSA) can adopt different forms. For better understanding of the pH effect onto the protein the Figure 3.3 illustrates the compaction of serum albumin in its N, F and E forms. Each form has its own value of pH and different rates of compression, so this parameter can affect the adsorbed amount of BSA onto the substrate [52].

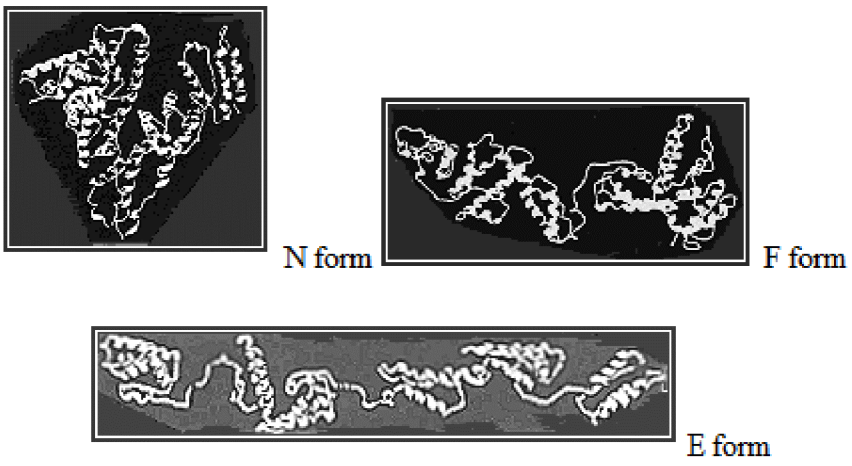

Figure 3.3: Representation of serum albumin in its N form, and in its proposed F and E forms (adapted from [52]).

According to Peters *et al.* [51] the Normal (N), Fast (F) and Expanded (E) transitions are involved in the unfolding of protein that varies according to different values of pH (Figure 3.4).

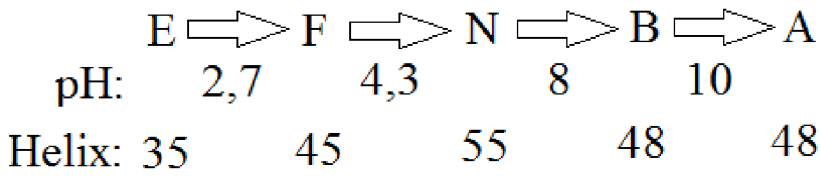

Figure 3.4: Relationship of isomeric forms of bovine serum albumin (adapted from [51]).

Each form has its specific properties. For example, F form is characterized by increase in viscosity, much lower solubility, and a significant loss in helical content. F-E transition occurs at pH < 4 and is accompanied by the loss of the intra-domain helices [51]. This form is characterized by high viscosity. Albumin at pH 9 changes conformation to the Basic (B) form. At pH 9, at low ionic strength, at 3°C and during 3 - 4 days it occurs the formation of Aged (A) form.

Experiment with HA

To study the variation of the zeta potential of hydroxyapatite as a function of pH, the substrate (0.2 g/L) was immersed in distilled water for 1 day. The measurement of the pH was carried out for two different temperatures: 25ºC and 36ºC. These values were chosen because 25 ºC is the room temperature and 36 ºC is the approximate temperature of the human body, usually taken as 37 ºC. This temperature was reached in about 1h30 min, but due to the loss of heat during the measurement of pH, a difference of 1 ºC was always observed.

The zeta potential measurements at 25 ºC and 36 ºC as a function of pH are represented in Figure 3.5. From the point of view of practical importance the difference between the temperatures is not significant. This affirmation was confirmed by the ANOVA statistical test ($p=0.69$). Since solubilization of the different materials showed to be easier for the higher temperatures, we used the temperature of 36ºC.

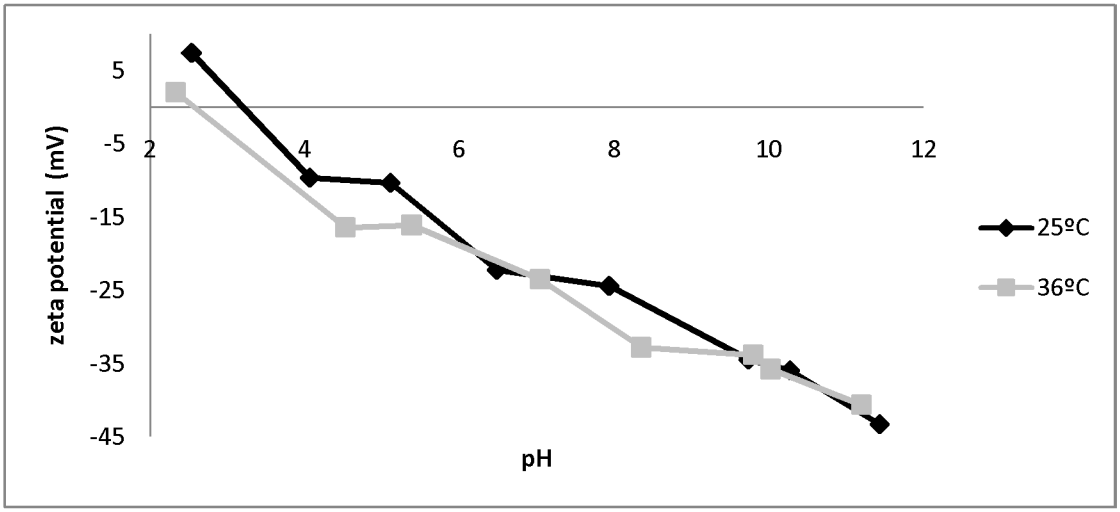

Figure 3.5: The zeta potential measurements of HA (0.2 g/L) at 25ºC and 36ºC after 1 day of immersion as a function of pH.

Another experiment was made to compare the zeta potential variation as a function of pH in two different media: water and PBS (Figure 3.6). This experiment was undertaken to understand the importance of buffered solution in zeta potential measurements in comparison with water. In both cases HA was used in a concentration of 0.2 g/L at 36ºC after 1 day of immersion.

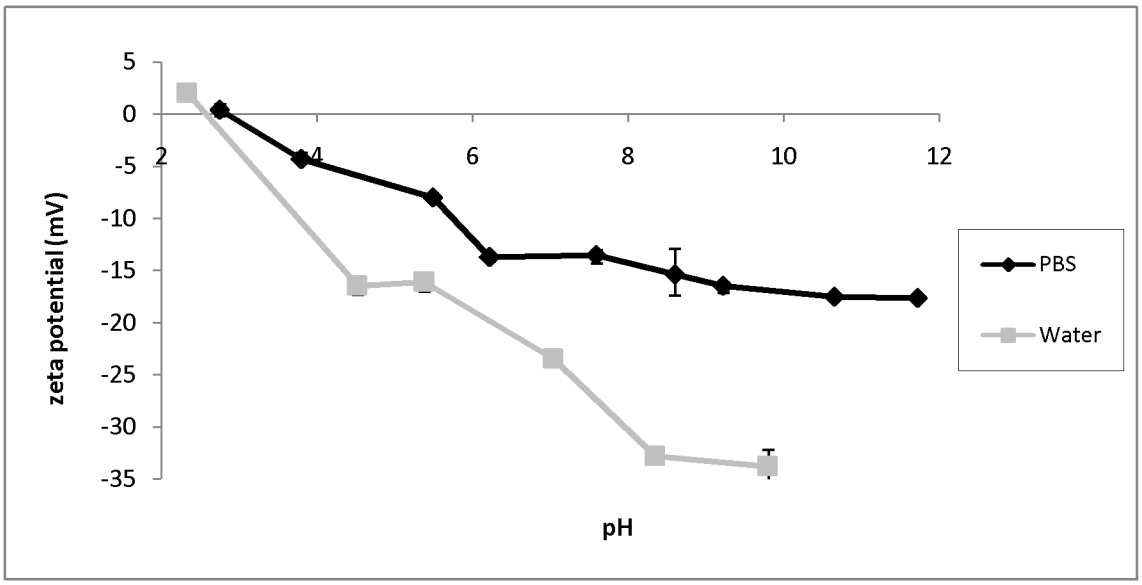

Figure 3.6: Zeta potential of HA (0.2 g/L) as a function of pH after 1 day of immersion in water or PBS (Table 4, Experiment Group A).

It should be noted that the curve of HA zeta potential in function of pH in PBS is different from the one obtained in water. Figure 3.6 illustrates that the surface charge of the HA is more positive in the PBS solution than in water. The results also indicate that for values of pH above the isoelectric point (pH≈2.8), colloidal

solution becomes less stable when using PBS buffer solution. With increase of pH the zeta potential decreases more in the water than in PBS, so the concentration of OH^- ions is higher in water than in the buffer solution. This phenomenon can be explained by the existence of different cations around the ionic layer. In the case of water the unique cation are protons H^+. It is a small particle comparing with the salts from PBS (Na^+, K^+). Na^+ has 194 pm in diameter and K^+ has 244 pm against the H^+ that has 0.8 fm [93]. So in PBS solution the ionic layer suffers more force of compression and the zeta potential increases.

It is possible to mark two more conditions that can affect the surface charge. The electrical charges on the aqueous oxide surface are transferred to the protonation (eq.4) or deprotonation (eq.5) of the hydroxyl surface and have the following reaction equation [93].

$$-ROH + H^+ = MOH_2^+ \qquad \text{eq.4}$$

$$-ROH + OH^- = -MO^- + H_2O \qquad \text{eq.5}$$

Figure 3.7 represents the results of HA zeta potential measurements as a function of pH from the present work, from Yin *et al.* [94] and from Ribeiro *et al.* [95]

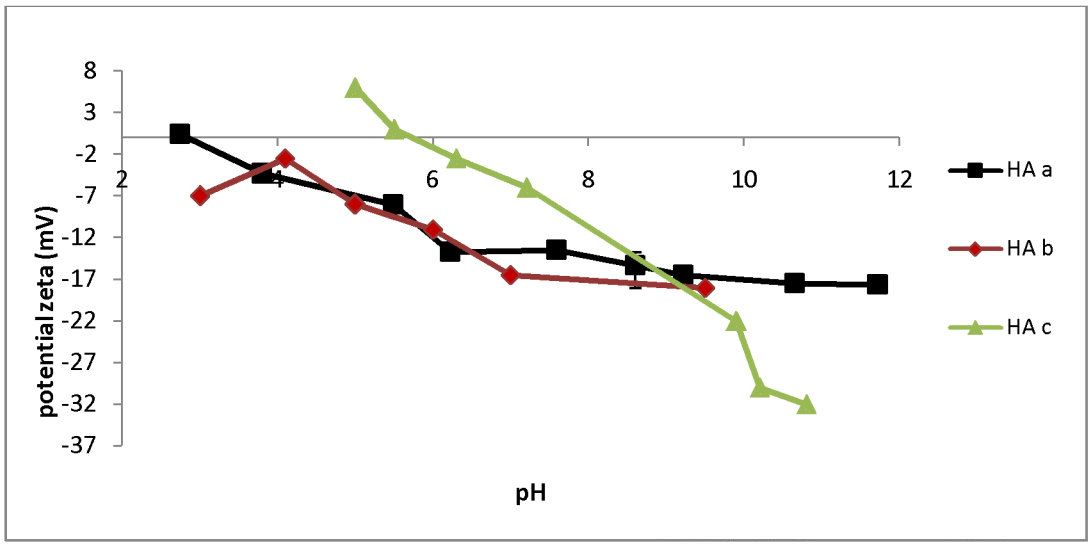

Figure 3.7: HA Zeta potential as a function of pH: a) Results from the present work (0.2 g/L, PBS, T=36 ºC 1 day of immersion - Table 4, Experiments Group A); b) Results from Yin *et al.* (PBS, T=18.5ºC) and c) Results from Ribeiro *et al.* (PBS, D_a<20.51 µm)

Current work showed that the IEP for HA is located at pH≈2.8. This condition indicates that the surface of the material is more positively charged in acid

suspensions and the suspension is more stable for high pH values. When reducing the zeta potential, the distance between the particles can be reduced and this condition increases the probability of their collision [93]. In this work the time of immersion of HA in PBS was 24h. Although PBS is not a very aggressive medium, it is likely that some apatite precipitates have formed after 24 hours on the HA particles. This condition can influence the value of the true HA surface charge.

The results from Yin *et al.* [94] have the particularity of showing that HA particles are negatively charged in the whole pH range from 3-10 with no IEP in this range. The decrease in HA zeta potential is observed for pH value increasing from pH 4.0, indicating the enhanced adsorption of anions on HA surface, probably OH^- in PBS. The study of Yin *et al.* [94] does not specify the values of particle size but TEM images in the paper show that the experiments were made with nano-HA. Zeta potential measurements were performed at 18.5ºC. Due to the different experimental conditions, a reliable comparison with the results of the present work is not straightforward.

The experimental work by Ribeiro *et al.* [95] was carried out with HA particles smaller than 20.51 µm in PBS buffer solution and led to an isoelectric point at pH 6. At physiological pH (7.4) the surface of HA used by these authors is less negatively charged compared to the results obtained for the same pH in this work. For pH below 9 the surface of HA in the current work has more negative surface charge than the HA particles from Ribeiro *et al.* [95] but for basic suspensions HA particles from this work have higher zeta potential.

Tian *et al.* [96] measured the zeta potential of two different types of HA nanoparticles to study the dependence of their surface charge on the preparation technique. The results are shown in Figure 3.8 for hydroxiapatite HA1 synthesized by chemical precipitation, and HA2, which was derived from HA1 by calcination at 900ºC during 24 h.

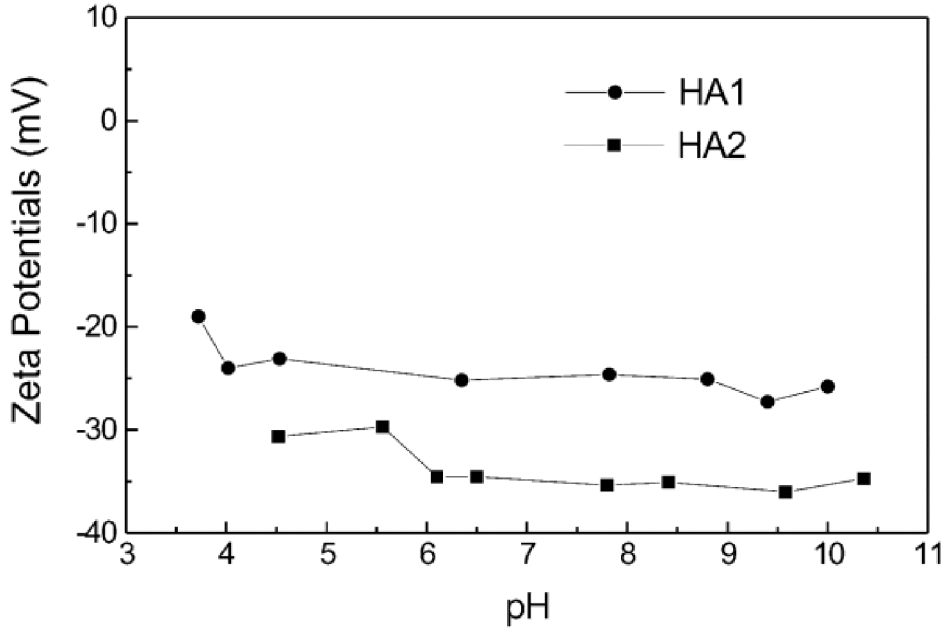

Figure 3.8: Zeta potential measurements of HA as a function of pH [96].

Surface charge of these materials is significantly lower than for all the other HA powders referred. It is not clear whether the effect of preparation can explain the observed trend and the low surface charges. After the calcination the particle size of HA1 changed from 65 nm to 115.1 nm for HA2 [96].

Experiments with Bioglass V7

The process of immersion of a bioactive glass in an aqueous solution is accompanied with ions dissolution from the glass (such as Na+). For the 45S5 bioactive glass, Hench [87] showed that at the early stages the dissolution process is followed by the formation of a silica-rich surface layer.

Zeta potential measurements in a glass suspension may be influenced by this dissolutioin process. As the time for zeta potential measurements is usually short, the surface layer should not undergo significant alterations. If additional changes occur, such as the formation of a calcium phosphate material on the surface of the glass particles, then changes in the zeta-potential values might be expected.

Qiang *et al.* [87] reported the work carried out with a silica-based bioglass of composition $53SiO_2$, $6Na_2O$, $12K_2O$, $5MgO$, CaO, $4P_2O$, designated by 13-93 glass. Zeta potential at different pH values was measured in a suspension of this glass (average particle size of 2 μm) in PBS. Figure 3.9 represents these results together with the results for the bioglass V7 studied in the present work.

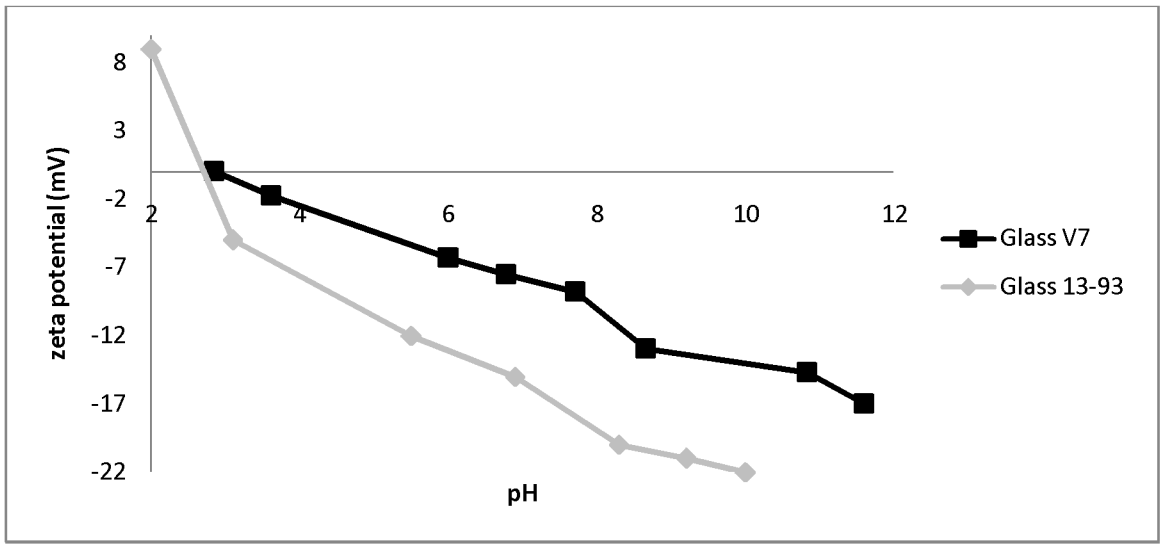

Figure 3.9: Zeta potential as a function of pH for bioglass V7 (Table 4, Experiments Group E) and for the13-93 glass [87] (PBS, D_a= 2 μm).

The curves of zeta potential are situated more in the negative area because the OH^- ions are probably the predominant surface species. The IEPoints for the 13-93 bioglass and for the bioglass V7 are located, respectively, at pH=3 and at pH= 2.85. For both glasses the zeta potential decreases with the increase of pH. It is observed that the surface charge of bioglass V7 is more positive than the one of the 13-93 bioglass for values of pH higher than the IEP. It is reported in the paper that the median size of the 13–93 glass particles was 2 μm. The average size of V7 glass was 2.73 μm. Qiang *et al.* [87] do not refer the values of immersion time and of temperature used.

Experiments with PLLA

To our knowledge no zeta potential measurements for PLLA powders have been reported yet. To compare the surface charge behavior of PLLA with other biocompatible polymers, data for Polythene (PE) [35] and for poly (α-methacrylic acid)-grafted polylactide (PMAA-PLA) [97] polymers were used.

Figure 3.10 represents the zeta potential measurements for suspensions of PLLA, PE and PMAA-PLA as a function of pH. Among the three materials studied in this project, PLLA showed the highest variation in zeta potential values (from -29 mV to 11.57 mV). The IEP of PLLA corresponds to the pH value of 4.1.

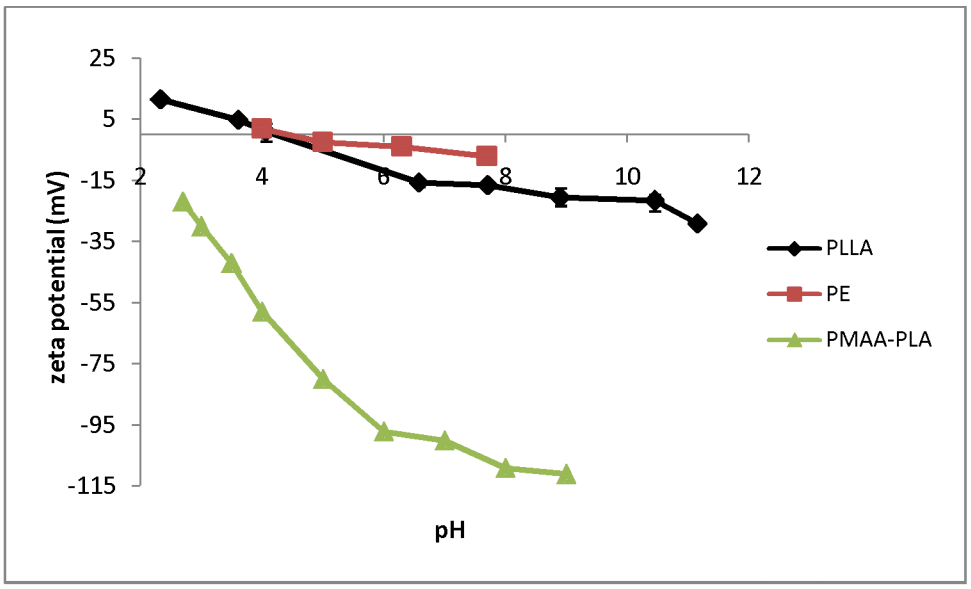

Figure 3.10: Zeta potential as a function of pH for PLLA (Table 4, Experiments Group I), PE (35) (PBS)) and PMAA-PLA [97] (PBS, D_a=172.8 nm)).

The zeta potential for pure PE varies from 1.7 to −5.2 mV with an isoelectric point at pH 4.5 (Figure 3.10). The representation also shows that PLLA has more negative charged surface than PE, so PLLA gives rise to more stable colloidal

suspensions than PE, although they have similar localization of IEP. Temperature, particle size and immersion time are not specified by Xu *et al.* [35].

The great difference between the surface charges of materials is due the difference in their structure (Figure 3.11) [98]. PE has small possibility to form ions on its surface while PLLA in alkaline medium can easily break the double bond between carbon and oxygen to form O^-. In other words, the carboxyl groups of PLLA surfaces could ionize into COO^- with negative charge in alkaline solution.

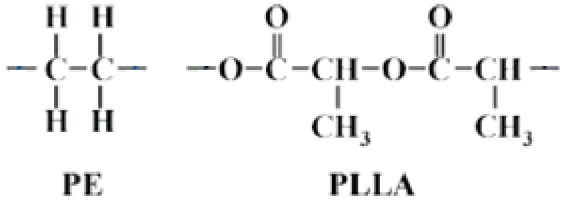

Figure 3.11: Chemical structure of PE and PLLA monomers (adapted from [98])

The results of zeta potential measurements of PMAA-PLA microparticles (172 nm) presented by Xiao *et al.* [97] show higher surface negative charge (Figure 3.10) than those obtained for PLLA in this work. Xiao *et al.* [97] do not detail parameters such as temperature, medium and immersion time. The average particle size of PMAA-PLA was 172.8 nm and of PLLA - 4.68 µm.

Comparison of HA, Bioglass V7 and PLLA zeta potential measurements

Figure 3.12 represents the zeta potential measurements of HA, bioglass V7 and PLLA powders (0.2 g/L in PBS at 36 ºC) as a function of pH after 1 day of immersion at the conditions of the experiment. It is observed that, although having the same IEP (pH≈ 2.8 for HA, pH≈2.85 for V7), HA has a more negative surface charge than bioglass V7 in the whole range of pH studied. The surface of PLLA is more positively charged than the two other substrates until pH= 5.5. This behavior on the surface of the PLLA material can be explained by the predominant concentration of ions (OH^-) in the solution.

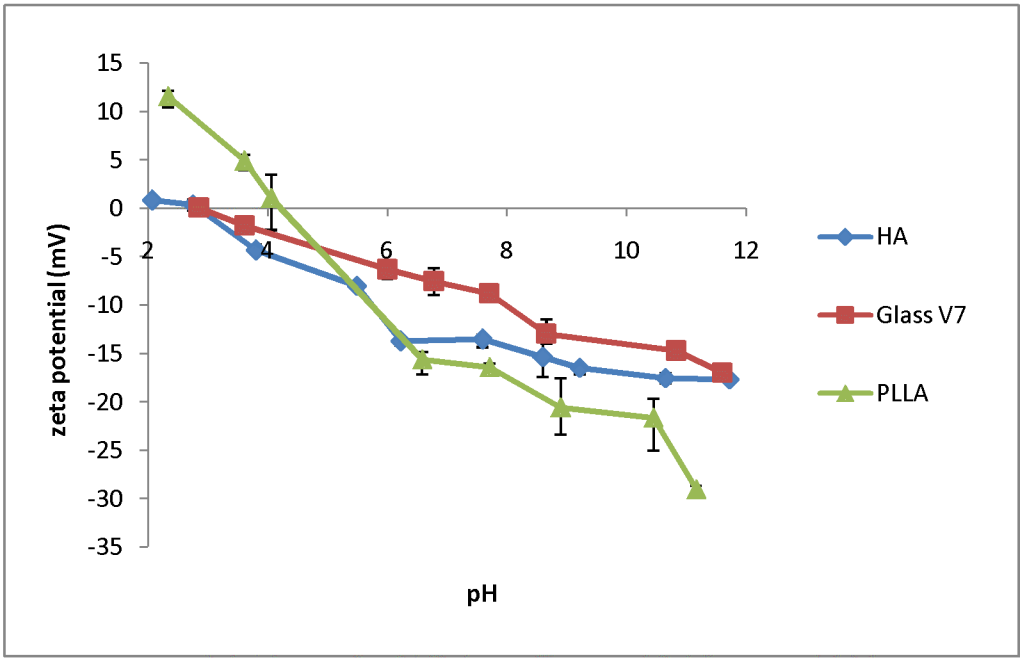

Figure 3.12: Zeta potential as a function of pH for HA, glass V7 and PLLA powders (Table 4, Experiments Groups A, E and I respectively) (0.2 g/L in PBS after 1 day of immersion).

One of the reasons why HA has the negative surface charge at pH 5.0 is the predominance of $H_2PO_4^-$ ions on its surface. At pH 7.0 the surface charge of HA decreases due to the increased HPO_4^{2-} and $H_2PO_4^-$ ions concentration.

5.2. BSA quantification vs pH

Figure 3.13 represents the adsorbed quantities of BSA on particles of HA, glass V7 and PLLA (0.2 g/L in PBS) as a function of pH.

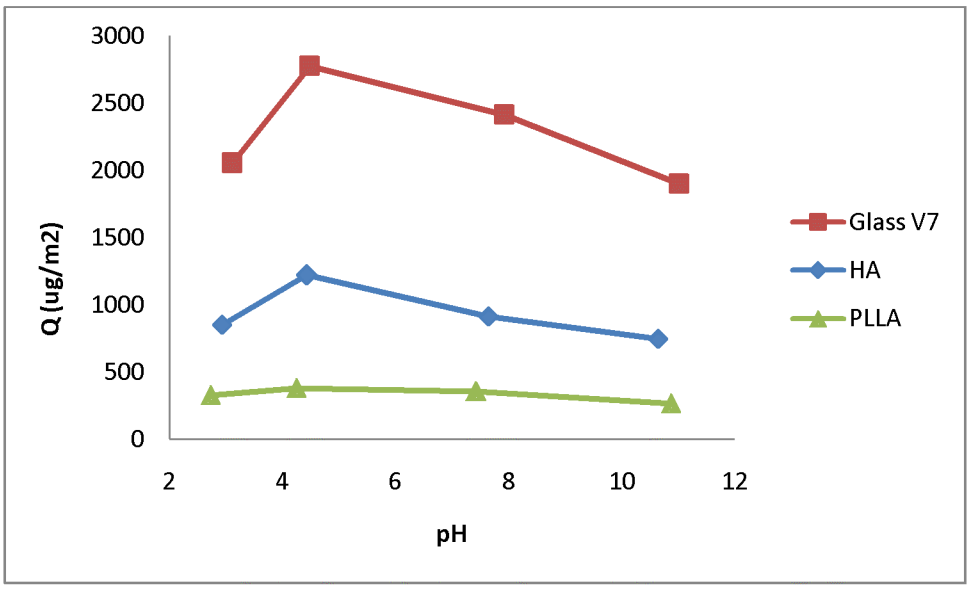

Figure 3.13: Adsorbed quantity of BSA as a function of pH onto HA, glass V7, and PLLA powders (Table 5, Groups A, D and G respectively)

The leader of adsorbed quantity of BSA among the used materials is the bioglass V7. This substrate has an IEP of 2.85 lower than the BSA IEP, 4.7, so the big interval between IEPs of the material and of the protein is more favorable for the BSA adsorption. In other words this means that the better interval for BSA adsorption corresponds to the situation when the surface charges of the material and of the protein have opposite signs. In this case the substrate has negative sign and the protein has positive sign.

HA particles adsorb less amount of protein than bioglass V7 even having similar IEPs (2.8 for HA and 2.85 for V7). According to Figure 3.12 the HA surface is more negatively charged than the bioglass V7 surface, and thus a simple analysis would suggest that HA should adsorb more BSA than V7. It should be pointed out here that the zeta potential measurements represented in Figure 3.12 were performed on particles soaked for 24 hours in PBS. Even admitting that PBS is not an aggressive medium it is quite probable that some apatite has precipitated onto the glass particles (more surface reactive than HA), thus creating a surface situation different from the one existing in the BSA quantification tests. In this case the as-prepared particles were immersed in the solution with 0.33 g/L BSA without previous incubation.

The substrate that has the lower amount of BSA adsorbed is PLLA. As shown in Fig 3.12 this material has more negatively charged surface than the other materials at high pH, so this parameter alone does not explain the difference in adsorbed BSA. The argument of apatite precipitation onto PLLA surface is not plausible in this case since PLLA is not a bioactive material.

The adsorption behavior of BSA onto materials surface should have a tendency to be higher for pH values lower than the isoelectric point of BSA (4.7) due to the electrostatic affinity interaction between BSA with positive charges and

the material with negative charges. In the present work the IEP of PLLA is 4.1, which is close to the IEP of BSA at pH=4.7. The interval where surfaces have different signs charges is very small. Another factor to take into consideration in this discussion is related with the fact that BSA can adopt different conformations at different pH (see Section 5.1 Figure 3.3). At low values of pH the albumin has an "Extended" form and this can prevent the process of adsorption. For pH higher than 7.3 the electrostatic repulsion force between the material and BSA is increasing and it can inhibit even more the adsorption of BSA on the material. Only a deep study on the local electrical characteristics of the adsorbed protein can clarify the observed amounts of adsorbed BSA.

Yang *et al.* [99] reports that quartz crystal microbalance technique (QCM) measurements showed that the increase of pH value was unfavorable for the adsorption of BSA between pH of 4 and 8 for hydroxyapatite.

5.3. Substrate and BSA zeta potential as a function of pH

Experiments with HA substrate

Figure 3.14 represents the zeta potential measurements of HA as a function of pH (immersion time of one day) with and without the addition of albumin (0.33 g/L).

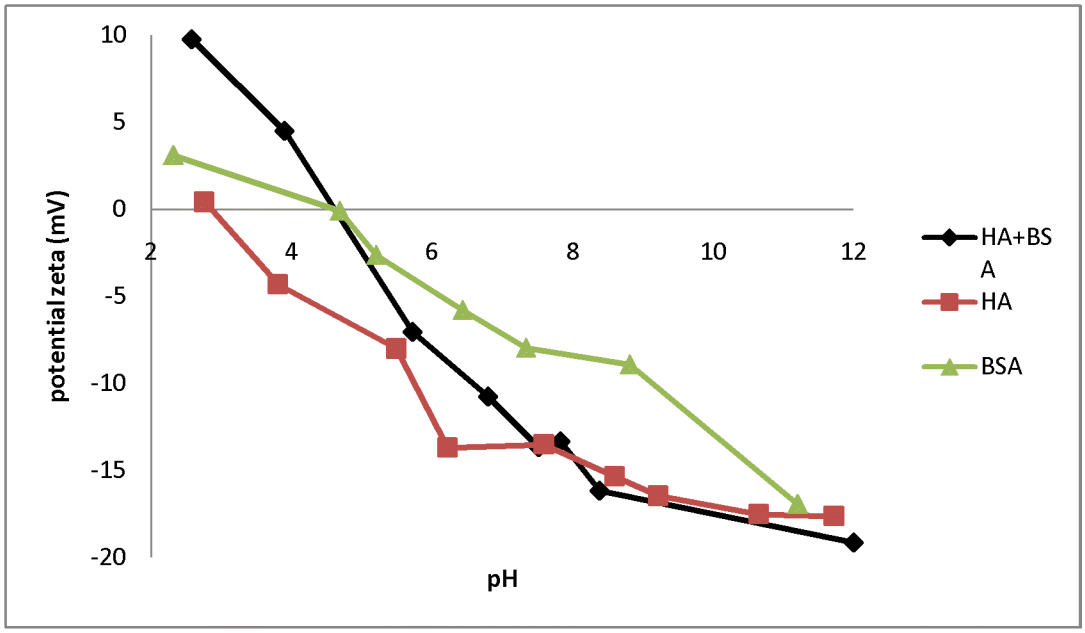

Figure 3.14: Zeta potential versus pH for HA, HA with adsorbed BSA (Table 5, Groups A and B respectively) and BSA (0.33 g/L) after 1 day of immersion time.

As referred before the IEP of hydroxyapatite is located at pH=2.8 and the IEP of HA with BSA adsorbed is situated between pH=4.5 and pH=4.8. It is interesting to notice that the IEP of BSA and of HA with adsorbed BSA are very similar. Since

HA powders have adsorbed BSA the Zetasizer measures the value of zeta potential of BSA.

The surface with albumin is more positively charged in acid suspensions. The suspension without added albumin is more stable between pH ≈ 3.5 and 8 than with adsorbed protein. Above pH 8 the surface with albumin becomes more negatively charged. This phenomenon probably occurs due to the dissociation of the main basic amino-type $R\text{-}NH_3^+$ with the release of OH^- in albumin. In alkaline solutions, this process suppresses and dissociates primarily carboxyl groups $RCOO^-$ with the release of H^+. When reducing the zeta potential, the distance between the particles can be reduced and this increases the probability of their collision.

Experiments with Bioglass V7 substrate

Figure 3.15 represents the zeta potential measurements of bioglass V7 as a function of pH with and without addition of albumin (0.33 g/L) after 1 day of immersion time.

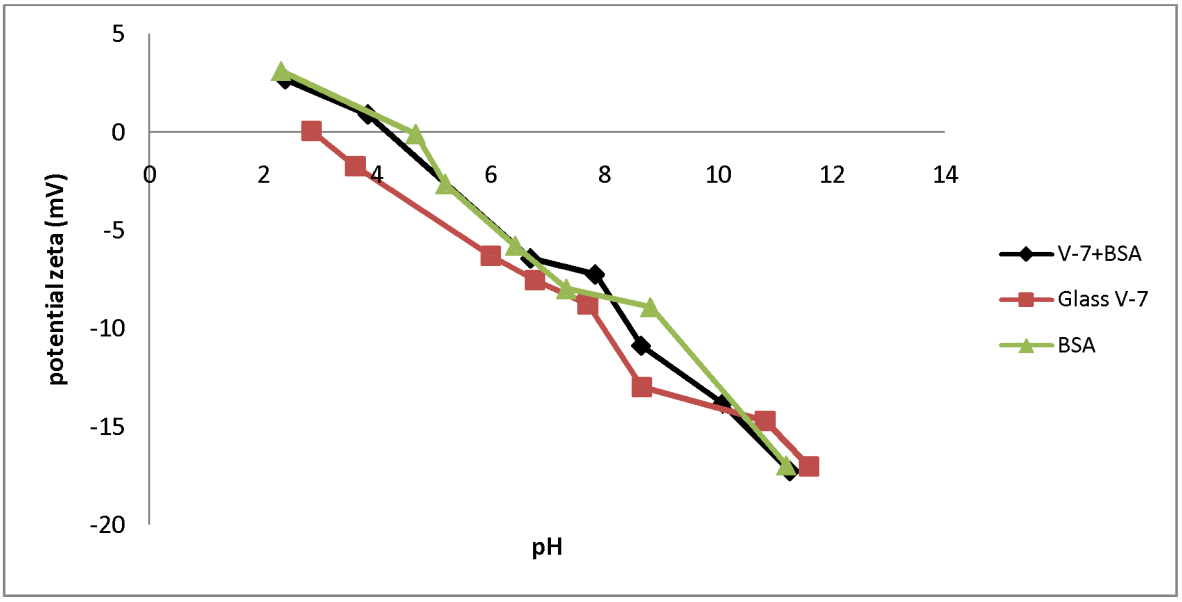

Figure 3.15: The zeta potential measurements of bioglass V7, V7 with BSA adsorbed (Table 4, Groups E and F respectively) and BSA (0.2 g/L) after 1 day of immersion time as a function of pH.

The IEP of bioglass V7 (0.2 g/L) is around pH ≈ 2.85 against the IEP of the bioglass V7 with adsorbed BSA that is around pH ≈ 3.84. In this case the IEP for the bioglass and for the bioglass with adsorbed BSA are not the same but are close. The surface with albumin is more positively charged in acid suspensions. The suspension without added albumin is more stable between pH ≈ 3.5 and 10 than with adsorbed protein. Above pH 10 the surface with albumin becomes more negatively charged. The surface charge of protein adsorbed is positive in acid medium and becomes negative for the basic one.

It should be noticed that the similar behavior of HA and Bioglass V7 (Figure 3.14 and 3.15) after BSA adsorption is an indication that BSA has adsorbed onto their surfaces, thus making their electrical behaviors very equivalent.

Experiments with PLLA substrate

Figure 3.16 represents the zeta potential measurements in function of pH of polymer PLLA with and without the addition of albumin (0.33 g/L) after 1 day of immersion time.

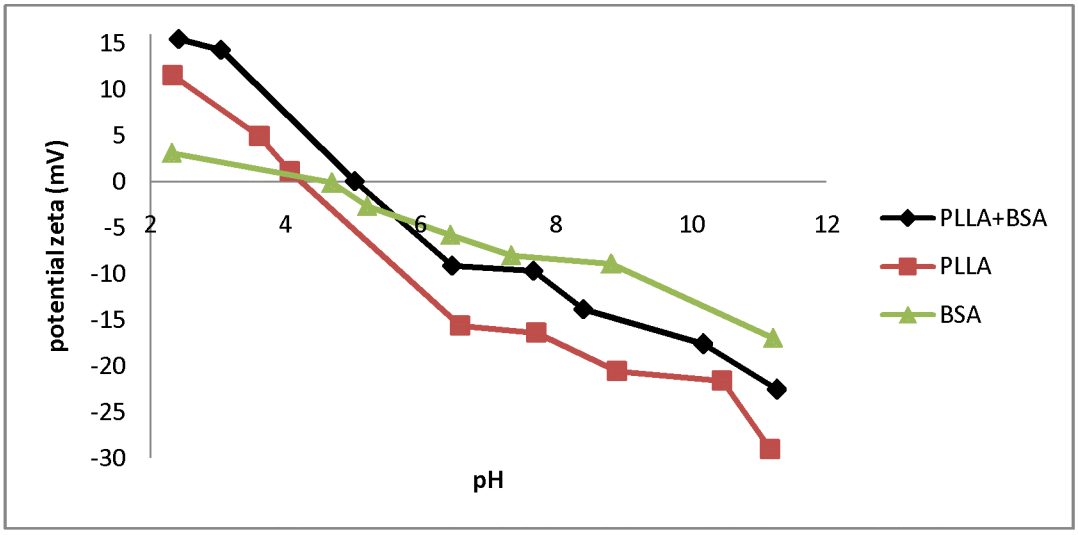

Figure 3.16: Zeta potential of PLLA, PLLA with adsorbed BSA (Table 4, Groups I and J respectively) and BSA (0.33 g/L) after 1 day of immersion time as a function of pH.

The IEP of the PLLA (0.2 g/L) is around pH ≈ 4.1 against the IEP of the PLLA with adsorbed BSA that is around pH ≈ 5.1. This behavior is similar to the one of bioglass V7, where the IEP of the substrate with protein adsorbed is close to IEP of BSA. For pH in the acid region the surface with adsorbed albumin is more positively charged.

5.4. The effect of BSA concentration

Figure 3.17 represents the HA, bioglass V7 and PLLA (0.2 g/L) variation of zeta potential according to the amount of albumin added to suspensions of these materials and kept for 100 h at pH=7.7.

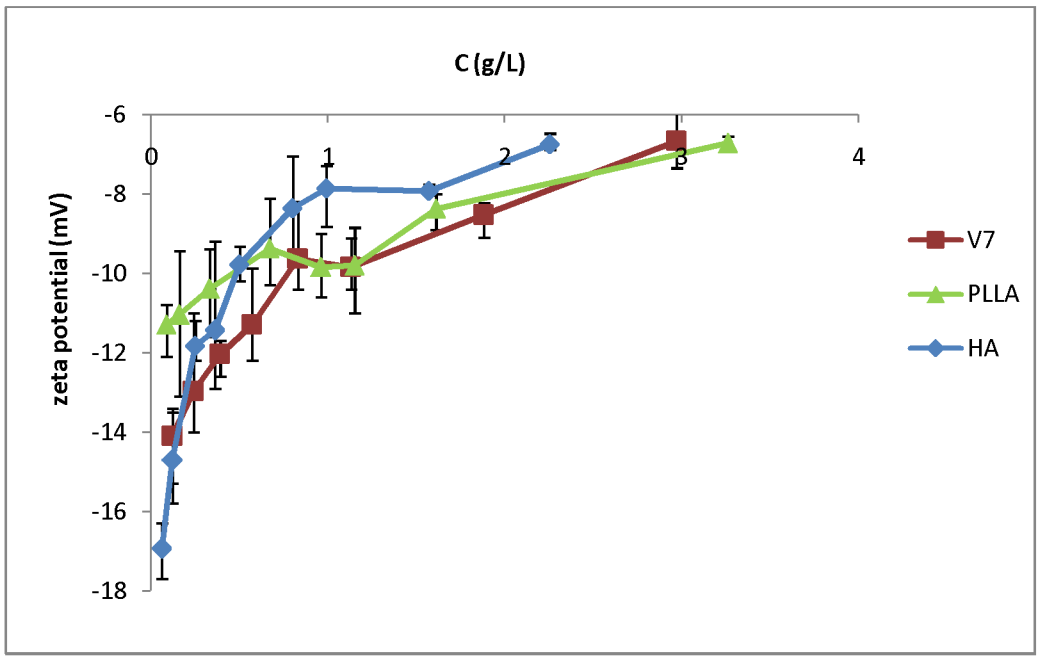

Figure 3.17: Variation of HA, V7 and PLLA zeta potential with the amount of added albumin after 100 h at pH=7.7 (Table 4, Groups D, H and L respectively).

For small concentrations of BSA the bioglass V7 has more positively charged surface than PLLA but from C= 2.5 g/L this phenomenon is inverted.

It can be observed that HA is the material with higher variation of surface charge with BSA concentration in the suspensions. The material for which the surface charge has the lower variation is PLLA.

For a better understanding of the observed differences in the behavior of the materials towards BSA adsorption, the next graphs represent the relationship between adsorbed quantity of BSA and the BSA concentration in PBS

Figure 3.18 represents the adsorbed quantity of BSA (0.33 g/L) as a function of protein concentration using HA, glass V7 and PLLA powders in PBS (0.2 g/L).

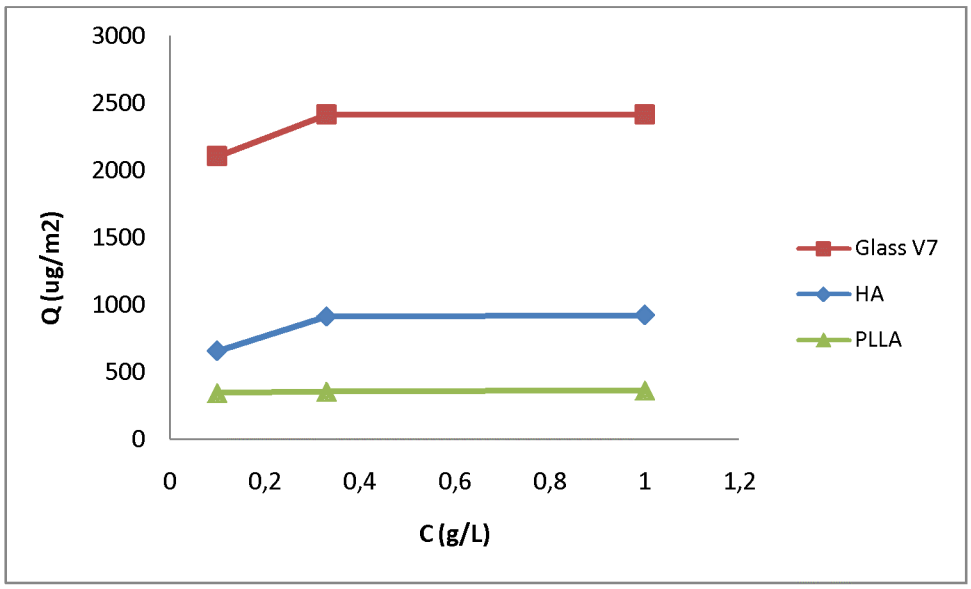

Figure 3.18: Dependence of adsorbed quantity of BSA on the concentration of the protein using HA, glass V7 and PLLA powders (Table 5, Groups B, E and H respectively).

It is observed that for the three materials studied in this project the amount of adsorbed albumin increases for the first concentratrion 0.33 g/L and becomes stationary for higher BSA concentrations. The capability of the materials to accept the protein is only evident for the lower BSA concentratrions. Bioglass V7 is the material that adsorbed more protein.

From Figure 3.17 it is shown that with increase of the BSA concentration the surface charge of all materials becomes less negative, which influences the electrical interaction with BSA in the suspensions. Also in this Figure, HA presents the largest variation of zeta potential as a function of BSA concentration but variation of adsorbed quantity with BSA concentration (Figure 3.18) is similar to the one for the other biosubstrates.

5.5. The effect of immersion time

Figure 3.19 represents the results of zeta potential measurements as a function of the immersion time using HA, glass V7 and PLLA powders (0.2 g/L).

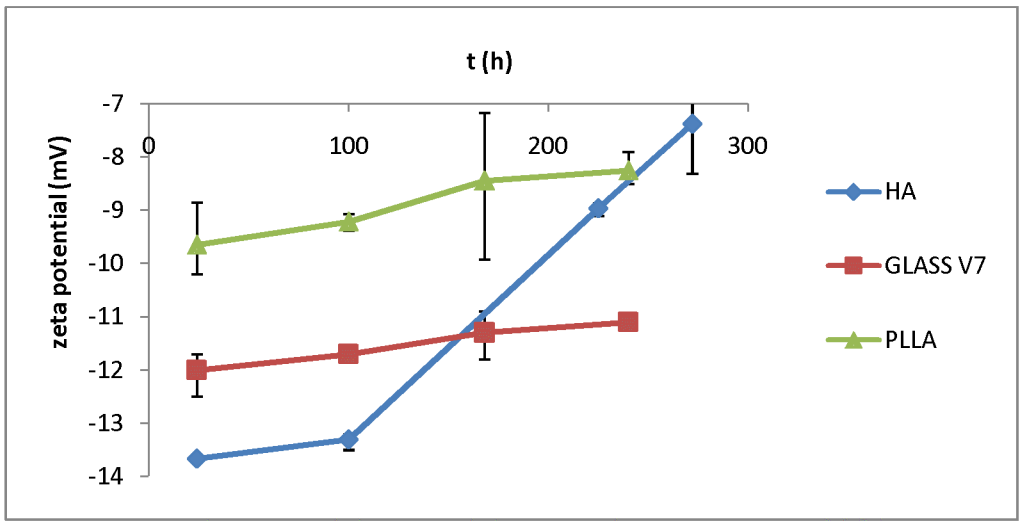

Figure 3.19: Dependence of zeta potential on immersion time using HA, glass V7 and PLLA powders (Table 4, Experiments Groups C, G and K respectively)

The variation of the surface charge of HA during the experience is the largest one. At the beginning the HA surface was the most negatively charged and after 300 hours it became the less negatively charged.

The relationship between the adsorbed quantity of BSA (0.33 g/L) and the immersion time is shown in Figure 3.20 for HA, glass V7 and PLLA powders (0.2 g/L).

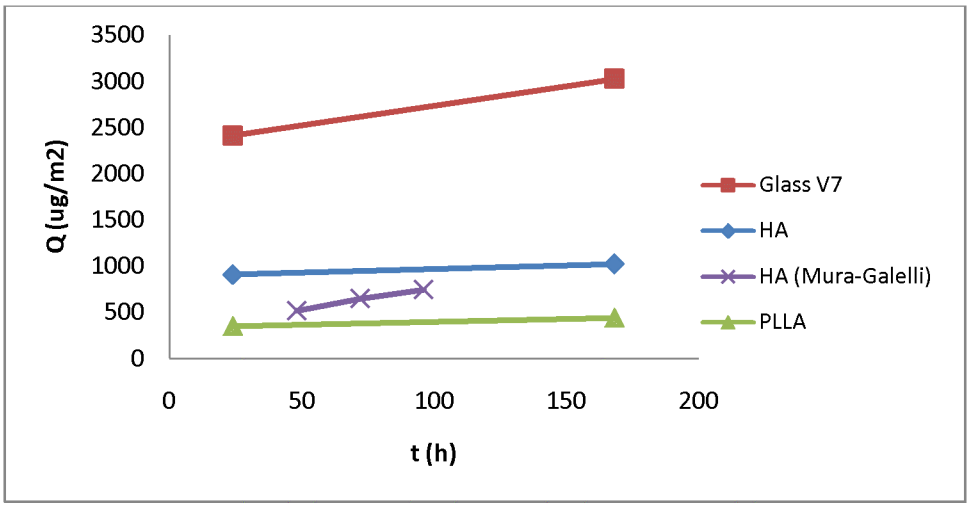

Figure 3.20: Dependence of adsorbed quantity of BSA (0.33 g/L) on immersion time using HA, glass V7, PLLA powders (Table 5, Experiments Groups C, F and I respectively). Results from Mura-Galelli *et al.* [100] are also shown.

Time seems to scarcely affect the amount of adsorbed protein onto HA and PLLA particles. Only for the glass V7 the amount of BSA has a significant increase with the soaking time.

Mura-Galelli *et al.* [100] studied the adsorption of human serum albumin (HSA) onto HA surface at pH 7.35. The data correspond to the line (HA (Mura-

Galelli) in Figure 3.21 that illustrates the dependence on immersion time of the adsorbed quantity of HSA onto HA. The results show that the quantity of adsorbed HSA increases with time within the time interval studied and that equilibrium is not attained even after 100 h of soaking time.

The amount of adsorbed HSA onto HA particles obtained by Mura-Galelli *et al.* [100] differs from the one obtained in the present work, although this work has been made with BSA. While Mura-Galelli *et al.* obtained 520 $\mu g/m^2$ HAS after 50 h of immersion, in the present work we obtained 900 $\mu g/m^2$ BSA after 24 h of immersion. Besides the difference in the proteins, other parameters can explain the observed differences, such as: (i) temperature, not specified in Mura-Galelli *et al.* paper and 36ºC in this work (ii) particles size (3.34 μm in the present study vs. 100-160 μm used by Mura-Galelli *et al.*), or (iii) surface electrical characteristics of the HA powders, specified in this work by the zeta potential measurements but not referred by Mura-Galelli et *al.*

6. Conclusions

The main purpose of this work was the study of the surface charge and its effect on the protein adsorption onto the surface of three materials: HA, a bioglass V7 and PLLA. Surface charge analysis was performed by zeta potential measurements (ZP) on particles of the required size and quantification of protein-BSA – was assessed by the modified Lowry method.

For all materials ZP was measured at 36 ºC, close to the temperature of the human body, and HA was also tested at 25ºC. The results of the experiments show that there is no significant difference in ZP values between the two temperatures.

The influence of the medium (PBS and distilled water) was evaluated for HA suspensions. The discrepancy found in the ZP measurements was explained by the different ions present in the medium.

Zeta potential measurements showed that PLLA is the material presenting the largest surface charge, with variation from 11.57mV (pH 2.33) to -29 mV (pH 11.16). The isoelectric point of this polymer is located at pH 4.1 that is close to the one for BSA (pH 4.7).

The zeta potential of HA varies from 0.42 mV (pH 2.75) to -17.63 mV (pH 11.72). HA has shown the more negative values of the electrical charge for the range of pH below 5.5.

Bioglass V7 exhibits the most positive surface charge in the range from 0,06 mV (pH 2.85) to -17 mV (pH 11.6) comparatively to the other materials studied. The isoelectric points of bioglass V7 and HA are similar (pH≈ 2.8 for HA and pH≈ 2.85 for V7) and lower than the one for BSA. However, differences in chemical composition between the surfaces of these materials could be responsible for this difference in zeta potentials.

ZP measurement for albumin indicated that it acquires positive charges at pH lower than 4.7, and above this pH value the surface is negatively charged. According to its isomeric forms (Figure 3.3) BSA performs different electrostatic interaction and aggregation states depending on the pH values.

ZP measurement of all materials was also carried out for different concentrations of BSA. The results for the materials with adsorbed BSA and for BSA alone showed similar isoelectric points. This phenomenon suggests that the adsorbed albumin tends to cover the material giving it a behavior similar to the one of protein alone.

The quantification of adsorbed BSA by the modified Lowry method indicate that the increase in pH from 4.7 is unfavorable for BSA adsorption for those materials whose IEP is lower than that of the BSA. Indeed different surface charge influence protein adsorption in different ways. Positive values of the ZP at fixed pH

indicate a positive charge of the surface, which will attract negatively charged entities such as anions or proteins. Negative charges of the materials surface tend to attract positively charged entities.

It was concluded that the bioglass V7 was the material that absorbed more quantity of BSA among all, even having the surface charge less negative than HA. PLLA is the polymer that adsorbed less amount of BSA.

Zeta potential measurements as a function of immersion time indicated that the surface charge of HA was mostly influenced by time among all materials. The bioglass V7 performed some variation of surface charge during the time of immersion, while PLLA is the material that exhibited less variation of surface charge on immersion time.

Only at high pH values the total charge of the surface with adsorbed BSA becomes more negative than the surfaces without protein. This affirmation is valid for HA and bioglass V7. In the case of PLLA and comparing with BSA curve the suspension without albumin added is more stable for more acid and basic values of pH.

References

[1] A cross-sectional study of bone turnover markers in healthy premenopausal women; *Anne E. de Papp, Henry G. Bone, Michael P. Caulfield, Risa Kagan, Anna Buinewicz, Erluo Chen, Elizabeth Rosenberg, Richard E. Reitz*; Bone 40 (2007) 1222–1230

[2] Bone markers and their prognostic value in metastatic bone disease: Clinical evidence and future directions; *Robert Coleman, Janet Brown, Evangelos Terpos, Allan Lipton, Matthew R. Smith, Richard Cook, Pierre Major*; Cancer Treatment Reviews (2008) 34, 629– 639

[3] Scaffolds a base de polimeros piezoelectricos para regeneração óssea; *Natália Braz Barroca*; Tese de Mestrado, Universidade de Aveiro *2008*

[4] Biochemical Markers of Bone Metabolism: An Overview; *Robert H. Christenson*; Clinical Biochemistry, Vol. 30, No. 8, 573–593, 1997

[5] Effects of Alcohol Use and Estrogen on Bone; *Russell T. Turner, Ph.D., and Jean D. Sibonga, Ph.D.*

[6] Dem bones, dem important bones; *Paul Clarkson*; August 2005

[7] Autologous Blood Transfusion in the Pediatric Patient; By Hannis W. *Thompson and Naomi L.C. Luban*; journal of Pediatric Surgary Vol30,No 10 (October),l995: pp 1406-1411.

[8] Potential of an ultraporous -tricalcium phosphate synthetic cancellous bone void filler and bone marrow aspirate composite graft; *E. M. Erbe, J. G. Marx, T. D. Clineff, L. D. Bellincampi*; Eur Spine J (2001) 10 :S141–S146

[9] The growing breast implant e a complication of homologous fat transplantation for breast augmentation; *Niklas Iblher, Vincenzo Penna, Department of Plastic Surgery, University, Medical Center, Matyas Bendek, Nikolaus Freudenberg, Department of Pathology, University Medical Center, G. Bjorn Stark, Department of Plastic Surgery, University Medical Center*; Journal of Plastic, Reconstructive & Aesthetic Surgery (2010) 63, e315ee316

[10] Structural changes in ceramic veneered three-unit implant-supported restorations as a consequence of static and dynamic loading; *Matthias Karla, Horst Fischerb, Friedrich Graefc, Manfred G. Wichmanna, Thomas D. Taylor, Siegfried M. Heckmanna*; dental materials 2 4 (2 0 0 8) 464–470.

[11] Implant fixation in knee replacement: Preliminary in vitro comparison of ceramic and metal cemented femoral components; *Luca Cristofolini, Saverio Affatato, Paolo Erani, Domenico Tigani, Marco Viceconti*; The Knee 16 (2009) 101–108.

[12] Relevance of collagen piezoelectricity to "Wolff's Law": A critical review; *Andrew C. Ahna, Alan J. Grodzinskyc*; Medical Engineering & Physics 31 (2009) 733–741

[13] Computational study of Wolff's law with trabecular architecture in the human proximal femur using topology optimization; *In Gwun Janga, Il Yong Kim*; Journal of Biomechanics 41 (2008) 2353–2361

[14] Boning up on Wolff's Law: Mechanical regulation of the cells that make and maintain bone; *Jan-Hung Chen, ChaoLiu, LidanYou, CraigA.Simmons*; Journal of Biomechanics 43 (2010) 108–118

[15] Stresses in the local collagen network of articular cartilage: a poroviscoelastic fibril-reinforced finite element study; *W. Wilson, C.C. van Donkelaar, B. van Rietbergen, K. Ito, R. Huiskes*; Journal of Biomechanics 37 (2004) 357–366

[16] Involvement of Different Ion Channels in Osteoblasts' and Osteocytes' Early Responses to Mechanical Strain; *S. C. F. Rawlinson, A. A. Pitsillides, and L. E. Lanyon*; Bone Vol. 19, No. 6 December 1996:609-614

[17] Wettability and surface charge of Si_3N_4–bioglass composites in contact with simulated physiological liquids; *M. Amarala, M.A. Lopesb, J.D. Santosb, R.F. Silva*; Biomaterials 23 (2002) 4123–4129

[18] Method for controlling organisms and material therefore, method for selective adsorption of proteins and material therefore, cement material and biomaterial; US Patent 6 777 214, (17 August 17 2000)

[19] Temporal zeta potential variations of 45S5 bioactive glass immersed in an electrolyte solution; *Helen H. Lu, Solomon R. Pollack, Paul Ducheyne*; Journal of Biomedical Materials Research Part A, 51(1) (2000) 80-87

[20] Biocompatibility of polymer implants for medical applications; *The Graduate Faculty of The University of Akron, Christopher M. Brendel*; August 2009

[21] Electrically Charged Hydroxyapatite Enhances Immobilization and Proliferation of Osteoblasts ; *Yuri Dekhtyar, N. Polyaka and R. Sammons*; IFMBE Proceedings, 2008, Volume 20, Part 2, 23-25

[22] A new biphasic osteoinductive calcium composite material with a negative Zeta potential for bone augmentation; *Ralf Smeets, Andreas Kolk, Marcus Gerressen, Oliver Driemel, Oliver Maciejewski, Benita Hermanns-Sachweh, Dieter Riediger and Jamal M Stein*; Head & Face Medicine 2009, 5:13

[23] Biomedical surface science: Foundations to frontiers; *David G. Castner, Buddy D. Ratner*; Surface Science 500 (2002) 28–60

[24] Biomaterials in Canada: The first four decades; *John L.Brash*; Biomaterials 26 (2005) 7209–7220

[25] Modern biomaterials: a review—bulk properties and implications of surface modifications; *Paul Roach, David Eglin, Kirsty Rohde, Carole C. Perry*; J Mater Sci: Mater Med (2007) 18:1263–1277

[26] Laser applications in surface science and technology; *Horst-Günter Rubahn*; B.G. Teubner 1996

[27] Modern surface technology; *Friedrich-Wilhelm Bach,Andreas Laarmann,Thomas Wenz*; Wiley-VCH 2004

[28] The anti-cell death FNK protein protects cells from death induced by freezing and thawing; *Kentaro Sudo, Sadamitsu Asoh, Ikuroh Ohsawa, Daiya Ozaki, Kumi Yamagata*; Biochemical and Biophysical Research Communications 330 (2005) 850–856

[29] Protein adsorption on surfaces: dynamic contact-angle (DCA) and quartz-crystal microbalance (QCM) measurements; *H. Stadler · M. Mondon · C. Ziegler*; Anal Bioanal Chem (2003) 375 :53–61

[30] Adsorption of poly(ethylene oxide)–*block*–polylactide copolymers on polylactide as studied by ATR-FTIR spectroscopy; *Štepan Popelka, Lud'ka Machova, František Rypacek*; Journal of Colloid and Interface Science 308 (2007) 291–299

[31] Fabrication methods of an engineered microenvironment for analysis of cell–biomaterial interactions; *Heungsoo Shin*; Biomaterials 28 (2007) 126–133

[32] On the Adsorption of Proteins on Solid Surfaces, a Common but Very Complicated Phenomenon; *Kazuhiro Nakanishi, Takaharu Sakiyama and Koreyoshi Imamura; Jornal of bioscience and Bioengineering*, Vol. 91, No. 3, 233-244. 2001

[33] Volumetric interpretation of protein adsorption: Competition from mixtures and the Vroman effect; *Hyeran Noh, Erwin A. Vogler*; Biomaterials 28 (2007) 405–422

[34] Bone response to surface-modified titanium implants: studies on the early tissue response to machined and electropolished implants with different oxide thicknesses; *C. Larsson, P. Thomsen, B.-O. Aronsson, M. Rodahl, J. Lausmaa, B. Kasemo and L.E. Ericson*; Biomaterials 17 (1996) 605-616

[35] A new insight into the adsorption of bovine serum albumin onto porous polyethylene membrane by zeta potential measurements, FTIR analyses, and AFM observations; *Tongwen Xu, Rongqiang Fu and Lifeng Yan*; Journal of Colloid and Interface Science 262 (2003) 342–350

[36] Basics of macroscopic properties of adsorbed protein layers, formed at air-water interfaces, based on molecular parameters; *Peter A. Wierenga*; Van Wageningen Universiteit (2005)

[37] Cell culturing: Surface aspects and considerations, in: J.L. Brash, P.W. Wojciechowski (Eds.); *T.A. Horbett, L.A. Klumb*; Interfacial Phenomena and Bioproducts, Marcel Dekker, New York, 1996, pp. 351–445.

[38] Adsorption of serum albumin on silica – The influence of surface cleaning procedures; *Olof Svensson, Thomas Arnebrant*; Journal of Colloid and Interface Science (2009).

[39] The relationship of interaction forces in the protein adsorption onto polymeric microspheres; *J.Y. Yoon, J.H. Kim, W.S. Kim*; Coll. Surf. A 153 (3) (1999) 413–419.

[40] A study on the adsorption of bovine serum albumin onto electrostatic microspheres: Role of surface groups; *Wuke Li and Songjun Li*; Elsevier B.V. (2006)

[41] Competitive adsorption of collagen and bovine serum albumin—effect of the surface wettability; *Peiqing Ying, Gang Jin, Zulai Tao*; Colloids and Surfaces B: Biointerfaces 33 (2004) 259–263.

[42] Interpretation of protein adsorption: surface-induced conformational changes; *P. Roach, D. Farrar, C.C. Perry*; J. Am. Chem. Soc. 127 (22) (2005) 8168–8173.

[43] Effect of pH and temperature on absorption desorption of Cu2+ in soil nearby a copper tailings yard; *Y.B.Wang, X.Q.Zhang*; 978-1-4244-4713-8/10/$25.00 ©2010 IEEE

[44] Wetting and spreading; *Daniel Bonn, Jens Eggers, Joseph Indekeu, Jacques Meunier and Etienne Rolley*; REVIEWS OF MODERN PHYSICS, VOLUME 81, APRIL–JUNE 2009

[45] Wettability and surface charge of Si_3N_4–bioglass composites in contact with simulated physiological liquids; *M. Amarala, M.A. Lopesb, J.D. Santosb, R.F. Silva*; Biomaterials 23 (2002) 4123–4129

[46] Effect of water activity on unfolding of adsorbed protein at the interface; *A. Shibata, Y. Iizuka, S. Ueno, T. Yamashita*; Thin Solid Films 284285 (1996) 549-551

[47] Manipulation of Hydrophobic Interactions in Protein Adsorption; *Robert D. Tilton, Channing R. Robertson, and Alice P. Gast*; *Langmuir* 1991, *7*, 2710-2718

[48] Coupled influence of substratum hydrophilicity and surfactant on epithelial cell adhesion; *Dewez JL, Schneider YJ, Rouxhet PG*; J Biomed Mater Res 1996; 30:373–83

[49] Cell adhesion to biomaterials: correlations between surface charge, surface roughness, adsorbed protein, and cell morphology; *Hallab NJ, Bundy K, O'Connor R, Clark R, Moses RL*; J Long-Term Effects Med Implants 1995; 3:209–31.

[50] Correlation between Body Weight and Serum Albumin Concentration in Premature Infants; *Shabih Manzar, Arun Kumar Nair, Mangalore Govind Pai, Saleh M Al-Khusaiby Neonatal Intensive Care Unit, Royal Hospital, Muscat, Sultanate of Oman*; Kuwait Medical Journal 2005, 37 (4): 248-250

[51] *Photocor Compact* – АНАЛИЗАТОР РАЗМЕРОВ И ДЗЕТА-ПОТЕНЦИАЛА НАНОЧАСТИЦ; АНТЕК-97; (2009)

[52] Antioxidant potential of anaerobic human plasma: Role of serum albumin and thiols as scavengers of carbon radicals; *Soriani M, Pietraforte D, Minetti M.*; Arch Biochem Biophys 1994; 312:180-188.

[53] http://gekrik.blogspot.com/2010/12/albumin.html (26.10.2010)

[54] Expectation-Maximization-Estimation of Mixture Densities for Electron-Spin-Resonance-Analysis of Albumin; *Christian Schmidt, Carsten Krumbiegel, Katja Waterstradt, Gabriele Petznick, Holger Schafer, Kerstin Schnurr*; IEEE GENSIPS, 2009

[55] Peters, T., Jr. (1985). Serum Albumin. *Adv. Protein Chem.*37; 161-245

[56] Quantitative Measurement of Adsorption of pH Dependent Structures Adopted by BSA; *Jian Lu, Biological Physics Group, School of Physics & Astronomy*, University of Manchester, UK.

[57] Albumin transport analysis of different collected and processed plasma products by electron spin resonance spectroscopy; *G. Matthes, G. Seibt, V. Muravsky, G. Hersmann, G. Dornheim*; Transfusion and Apheresis Science 27 (2002) 129–135

[58] Surface functionalized titanium thin films: Zeta-potential, protein adsorption and cell proliferation; *Kaiyong Cai, Marion Frant, J.org Bossert, Gerhard Hildebrand, Klaus Liefeith, Klaus D. Jandt*; Colloids and Surfaces B: Biointerfaces 50 (2006) 1–8

[59] Biomedical surface science: foundations to frontiers; *D.G. Caster, B.D. Ratner*; Surf. Sci. 500 (2002) 28–60.

[60] http://en.wikipedia.org/wiki/Zeta_potential; (26.10.2010)

[61] Zeta potential study of paste blends with slag; *Y. Elakneswaran, T. Nawa, K. Kurumisawa*; Cement & Concrete Composites 31 (2009) 72–76

[62] The Zeta Potential; Colloidal Dynamics Pty Ltd, Australian Technology Park, Colloidal Dynamics Inc, USA (1999)

[63] Electroflocculation: the effect of zeta-potential on particle size; *E. Ofir, Y. Oren, A. Adin*; Desalination 204 (2007) 33–38

[64] Nicomp 380 ZLS ; Appendix A PSS-ZLSM-042106 (11/06)

[65] Zeta potential of unexpanded and expanded perlite samples in various electrolyte media; *Mahir Alkan, O zkan Demirbas, Mehmet Dogan*; Microporous and Mesoporous Materials 84 (2005) 192–200

[66] Surface Chemistry and Surface Charge Formation for an Alumina Powder in Ethanol with the Addition of HCl and KOH; *J. Van Tassel and C. A. Randall*; Journal of Colloid and Interface Science 241, 302–316 (2001)

[67] Experimental and modeling investigation of sewage solids sedimentation based on particle size distribution and fractal dimension; *J. Wu; C. He;* Int. J. Environ. Sci. Tech., 7 (1), 37-46, Winter 2010

[68] Streaming potentials in chemically modified bone; *Otter M, Goheen S, Williams WS.*; J Orthop Res 1988;6(3):346–59.

[69] Preparation of hydroxyapatite ceramics for biomedical applications; *M. Haghbin Nazarpak, M. Solati-Hashjin and F. Moztarzadeh*; Journal of Ceramic Processing Research. Vol. 10, No. 1, pp. 54~57 (2009)

[70] Development and characterization of titanium-containing hydroxyapatite for medical applications; *J. Huang, S.M. Best, W. Bonfield, Tom Buckland*; Acta Biomaterialia (2010) 241–249

[71] Adsorption of bovine serum albumin onto hydroxyapatite; *Diana T. Hughes Wassell, Rachel C. Hall and Graham Embery*; Biomoterials16 (1995)697-702

[72] The interaction of proteins with hydroxyapatite. II. Role of acidic and basic groups; *Gorbunoff MJ.*; *Anal Biochem 1984; 136: 433-439*

[73] Impacts of the surface charge property on protein adsorption on hydroxyapatite; *Gang Yin, Zheng Liu, Jin Zhan, Fuxin Ding, Naiju Yuan*; Chemical Engineering Journal 87 (2002) 181–186

[74] The mechanism of biomineralization of bone-like apatite on synthetic hydroxyapatite: an *in vitro* assessment; *Hyun-Min Kim, Teruyuki Himeno, Masakazu Kawashita, Tadashi Kokubo and Takashi Nakamura*; *J. R. Soc. Interface* 2004 1, 17-22

[75] Adsorption of bovine serum albumin onto synthetic calcium hydroxyapatite: influence of particle texture; *Kazuhiko Kandori, Takashi Shimizu, Akemi Yasukawa, Tatsuo Ishikawa*; Colloids and Surfaces B: Biointerfaces 5 (1995) 81-87

[76] Synthesis, characterization and bioactivity investigation of bioglass/hydroxyapatite composite; *R. Ravarian, F. Moztarzadeh, M. Solati Hashjin, S.M. Rabiee, P. Khoshakhlagh, M. Tahriri*; Ceramics International 36 (2010) 291–297

[77] The story of bioglass; *L.L. Hench*; J. Mater. Sci. Mater. Med. 17 (2006) 967–978.

[78] Temporal zeta potential variations of 45S5 bioactive glass immersed in an electrolyte solution; *Helen H. Lu, Solomon R. Pollack, Paul Ducheyne*; Journal of Biomedical Materials Research Part A, 51(1) (2000) 80-87

[79] Improvement in toughness of poly(L-lactide) (PLLA) through reactive blending with acrylonitrile–butadiene–styrene copolymer (ABS): Morphology and properties; *Yongjin Li, Hiroshi Shimizu*; European Polymer Journal 45 (2009) 738–746.

[80] Bioresorbable Polymers in Or thopaedics; *David Farrar; Technology Manager for Biomaterials, Smith & Nephew Research Centre*

[81] Adsorption of serum albumin to thin films of poly(lactide-coglycolide); *Stephanie M. Butler, Mark A. Tracy, Robert D. Tilton*; Journal of Controlled Release 58 (1999) 335–347

[82] http://en.wikipedia.org/wiki/Polylactic_acid (7/05/2010)

[83] Phosphate Buffered Saline; SAGE In Vitro Fertilization, Inc. A CooperSurgical Company 95 Corporate Drive, Trumbull, CT 06611

[84] http://en.wikipedia.org/wiki/Phosphate_buffered_saline (26.10.2010)

[85]http://www.sigmaaldrich.com/catalog/ProductDetail.do?D7=0&N5=SEARCH_CONCAT_PNO|BRAND_KEY&N4=P3813|SIGMA&N25=0&QS=ON&F=SPEC (11.02.2011)

[86] http://en.citizendium.org/wiki/Henry%27s_law; (2.11.2010)

[87] Mechanical and in vitro performance of 13–93 bioactive glass scaffolds prepared by a polymer foam replication technique; *Qiang Fu, Mohamed N. Rahaman, B. Sonny Bal, Roger F. Brown, Delbert E. Day*; Acta Biomaterialia 4 (2008) 1854–1864

[88] Modified Lowry Protein Assay Kit; Thermo Fisher Scientific Inc (2008)

[89] Plant constituents interfering with the Lowry method of protein determination; *Jeffrey L. Smith*; Department of Botany and Microbiology, University of Oklahoma, Norman, Oklahoma 73019

[90] http://www.piercenet.com/files/lowry.pdf; (31.05.2010)

[91] Bioactive surfaces and biomaterials via atom transfer radical polymerization; *F.J. Xau, K.G. Neohb, E.T. Kang*; Progress in Polymer Science 34 (2009) 719-761

[92] Adsorption of albumin and IgG to porous and smooth titanium; *Eva Jansson, Pentti Tengvall*; Colloids and Surfaces B: Biointerfaces 35 (2004) 45–51

[93] Colloid Chemistry; *Fridrihsberg*; 1984

[94] Impacts of the surface charge property on protein adsorption on hydroxyapatite; *Gang Yin, Zheng Liu, Jin Zhan, Fuxin Ding, Naiju Yuan*; Chemical Engineering Journal 87 (2002) 181–186

[95] Calcium phosphate-alginate microspheres as enzyme delivery matrices; *C.C. Ribeiro, C.C. Barrias, M.A. Barbosa*; Biomaterials 25 (2004) 4363–4373

[96] Preparation and characterization of hydroxyapatite suspensions for solid freeform fabrication; *Jiemo Tian, Yong Zhang, Xinmin Guo, Limin Dong*; Ceramics International 28 (2002) 299–302

[97] Preparation and Cytocompatibility of Chitosan-Modified Polylactide; *Yumei Xiao, Dongxiao Li, Xuening Chen, Jian Lu, Hongsong Fan, Xingdong Zhang*; Wiley InterScience, 2008

[98] Modeling of the polyethylene and poly„L-lactide… triblock copolymer: A dissipative particle dynamics study; *Yao-Chun Wang, Wen-Jay Lee, and Shin-Pon Ju*; The Journal of Chemical Physics 131, 124901 _2009

[99] Adsorption/desorption behavior of protein on nanosized hydroxyapatite coatings: A quartz crystal microbalance study; *Zhengpeng Yang, Chunjing Zhang*; Applied Surface Science 255 (2009) 4569–4574

[100] Adsorption/desorption of human serum albumin on hydroxyapatite: A critical analysis of the Langmuir model; M. J. Mura-Galelli, J. C. Voegel, S. Behr, E. F. Bres, P. Schaaf; Biochemistry (1991)

Annex 1

Parameter	Experiments											
	Group A	Group B	Group C	Group D	Group E	Group F	Group G	Group H	Group I	Group J	Group K	Group L
pH	2.75	2.57	7.7	7.7	2.85	2.39	7.7	7.7	2.33	2.41	7.7	7.7
	3.8	3.89			3.62	3.84			3.61	3.04		
	5.49	5.72			6	6.7			4.06	5.02		
	6.22	6.79			6.78	7.84			6.58	6.46		
	8.6	7.51			7.71	8.65			7.71	7.66		
	9.22	7.82			8.66	10.09			8.9	8.4		
	10.65	8.38			10.83	11.27			10.45	10.17		
	11.72	12			11.6				11.16	11.26		
t (h)	24	24	24	100	24	24	24	100	24	24	24	100
			100				100				100	
			225				168				168	
			272				240				240	
BSA conc in PBS (g/L)	0	0.33	0.33	0.06	0	0.33	0.33	0.12	0	0.33	0.33	0.087
				0.12				0.24				0.16
				0.25				0.39				0.33
				0.5				0.57				0.67
				0.8				0.83				0.96
				0.99				1.13				1.15
				1.57				1.88				1.61
				2.26				2.97				3.26

Annex 2

<table>
<tr><th rowspan="2">Parameter</th><th colspan="9">Experiments</th></tr>
<tr><th>Group A</th><th>Group B</th><th>Group C</th><th>Group D</th><th>Group E</th><th>Group F</th><th>Group G</th><th>Group H</th><th>Group I</th></tr>
<tr><td rowspan="4">pH</td><td>2.93</td><td rowspan="4">7.6</td><td rowspan="4">7.6</td><td>3.11</td><td rowspan="4">7.7</td><td rowspan="4">7.7</td><td>2.73</td><td rowspan="4">7.7</td><td rowspan="4">7.7</td></tr>
<tr><td>4.43</td><td>4.48</td><td>4.24</td></tr>
<tr><td>7.64</td><td>7.92</td><td>7.42</td></tr>
<tr><td>10.64</td><td>11.01</td><td>10.87</td></tr>
<tr><td rowspan="2">t (h)</td><td rowspan="2">24</td><td rowspan="2">24</td><td>24</td><td rowspan="2">24</td><td rowspan="2">24</td><td>24</td><td rowspan="2">24</td><td rowspan="2">24</td><td>24</td></tr>
<tr><td>168</td><td>168</td><td>168</td></tr>
<tr><td rowspan="3">BSA conc in PBS (g/L)</td><td rowspan="3">0.33</td><td>0.1</td><td rowspan="3">0.33</td><td rowspan="3">0.33</td><td>0.1</td><td rowspan="3">0.33</td><td rowspan="3">0.33</td><td>0.1</td><td rowspan="3">0.33</td></tr>
<tr><td>0.33</td><td>0.33</td><td>0.33</td><td>0.33</td></tr>
<tr><td>1</td><td>1</td><td>1</td></tr>
</table>